minerals

MDPI

Review

A Review on Lithium Extraction Processes from Spodumene and Resource Utilization of the Generated Lithium Slag

Yongjie Bu [1,2,*], Wenxuan Yan [1,2], Xingxing Deng [3], Sen Huang [1,2], Aihui Sun [1,2], Qingjun Guan [1,2], Shuang Zhou [1,2], Wenqing Peng [1,2], Weijun Wang [1,2], Peng Ge [4] and Yue Yang [4]

1 School of Resource Environment and Safety Engineering, Hunan University of Science and Technology, Xiangtan 411201, China; 15370701869@163.com (W.Y.); 13639362873@163.com (S.H.); sunaihui@brunp.com.cn (A.S.); guanqingjun1@126.com (Q.G.); zhoushuang@hnust.edu.cn (S.Z.); pengwenqing@163.com (W.P.); wjwang@hnust.edu.cn (W.W.)
2 Hunan Province Key Laboratory of Coal Resources Clean-Utilization and Mine Environment Protection, Hunan University of Science and Technology, Xiangtan 411201, China
3 Key Laboratory of Sichuan Province for Lithium Resources Comprehensive Utilization and New Lithium Based Materials for Advanced Battery Technology, Chengdu 610041, China; cd.dengxx@tianqilithium.com
4 School of Minerals Processing and Bioengineering, Central South University, Changsha 410083, China; gp-gepeng@csu.edu.cn (P.G.); yangyue18@csu.edu.cn (Y.Y.)
* Correspondence: yongjie@hnust.edu.cn

Abstract

The booming new energy industry has fueled a surge in global lithium demand, with the annual demand for lithium carbonate (Li_2CO_3) equivalent (LCE) projected to reach 11.2 million tons by 2050. As a key raw material for lithium extraction, spodumene generates approximately 10–15 tons of lithium slag per ton of lithium carbonate (Li_2CO_3) produced. However, the comprehensive utilization rate of lithium slag in China remains below 30%, and most of it is disposed of through landfilling, posing soil pollution risks. This review summarizes the main lithium extraction processes from spodumene: the sulfuric acid method (with a lithium recovery rate of over 96% but high acid consumption); alkali processes (achieving 96%–99% lithium recovery and featuring low equipment corrosion, yet with untested applicability to low-grade ores); salt roasting (simplifying purification processes but only achieving ~60% sulfate recovery); and chlorination roasting (with a lithium recovery rate of over 95% but requiring strict safety controls). Additionally, this review covers the resource utilization of lithium slag: 8–10 million tons of gypsum can be recovered annually (filling 16%–20% of China's industrial by-product gypsum supply gap); the silica–alumina micro-powder can enhance concrete strength and reduce glass fiber production costs; and over 94% of tantalum (Ta) and niobium (Nb) can be recovered from fine tantalite concentrate slag. Key research gaps and future development directions are also identified to support the low-carbon development of the lithium industry.

Keywords: lithium; lithium extraction process; lithium slag; resource utilization; physicochemical properties

check for updates

Academic Editor: Hugo Marcelo Veit

Received: 15 September 2025
Revised: 3 October 2025
Accepted: 10 October 2025
Published: 14 October 2025

Citation: Bu, Y.; Yan, W.; Deng, X.; Huang, S.; Sun, A.; Guan, Q.; Zhou, S.; Peng, W.; Wang, W.; Ge, P.; et al. A Review on Lithium Extraction Processes from Spodumene and Resource Utilization of the Generated Lithium Slag. *Minerals* **2025**, *15*, 1073. https://doi.org/10.3390/min15101073

Copyright: © 2025 by the authors. Licensee MDPI, Basel, Switzerland. This article is an open access article distributed under the terms and conditions of the Creative Commons Attribution (CC BY) license (https://creativecommons.org/licenses/by/4.0/).

1. Introduction

With the booming development of the new energy sector, lithium—an essential strategic resource—has witnessed an explosive growth in demand [1]. Lithium and its compounds, renowned for their exceptional properties (e.g., high electrochemical activity, superior specific heat capacity, and outstanding redox potential) [2], are widely employed in batteries, ceramic glass, cement, pharmaceuticals, lubricants, the aerospace industry,

semiconductors, and other high-value fields [3]. These unique attributes have directly catalyzed the transformation of the electric vehicle industry, as lithium has become irreplaceable in lithium battery production, particularly for new energy vehicles. Key industrial lithium products encompass lithium carbonate (Li_2CO_3), lithium hydroxide (LiOH), and lithium chloride (LiCl), with lithium carbonate (Li_2CO_3) serving as the core material for new energy vehicle batteries [4]. According to forecasts from the Global Geology & Mineral Information Network, the global annual demand for lithium carbonate equivalent (LCE) is projected to reach 11.2 million tons by 2050 [5]. By then, the energy storage sector is anticipated to account for two-thirds of the total battery demand, underscoring lithium's critical role in the transition to a low-carbon economy. An increasing number of people recognize lithium's strategic importance, dubbing it "white gold" [6].

Lithium resources are abundant in nature and primarily categorized into brine-, hard-rock-, and clay-type [7]. The primary processes for lithium extraction encompass limestone calcination, sulfuric acid calcination, chlorination calcination, salt calcination, and alkali pressure digestion [8]. The physicochemical properties of lithium slag, a by-product generated during the lithium extraction process, vary depending on the specific extraction technology employed [9]. Quantitatively, approximately 10–15 tons of lithium slag are generated globally for every ton of lithium carbonate (Li_2CO_3) produced through spodumene ($LiAl(SiO_3)_2$) processing [10]. As the world's largest lithium-producing country, China has seen its annual lithium slag output exceed 120 million tons in recent years, with an annual new increment of about 10 million tons and a total historical stockpile reaching tens of millions of tons. However, its comprehensive utilization rate remains below 30% [11].

Currently, the disposal methods for lithium slag mainly involve land-filling or open-air stockpiling, resulting in low utilization rates. A small portion of lithium slag is used as a construction material [12], while the majority remains difficult to recycle and reuse effectively. The extensive stockpiling of lithium slag not only occupies land resources but also leads to soil pollution, as elements, such as the sulfur contained in the slag, are leached away with water and soil erosion. To address this practical challenge, multiple guidelines have been issued at the national level: the 14th Five-Year Plan for Circular Economy Development specifies that the comprehensive utilization rate of industrial solid waste should exceed 60% by 2025, and the revised Law on the Prevention and Control of Environmental Pollution by Solid Waste (2020) requires the management of lithium slag to be strengthened [13]. Therefore, the resource utilization of lithium slag has become a focus of national environmental protection and industrial policies. This paper provides a comprehensive overview of the sources, properties, and resourceful utilization of lithium slag and holds significant importance for the recycling and utilization of lithium slag. This paper follows a clear sequential structure: Section 2 focuses on lithium resource characteristics, elaborating on lithium occurrence forms and global spodumene distribution; Section 3 clarifies lithium slag sources by analyzing conventional spodumene lithium extraction processes (e.g., the sulfuric acid method and the alkali method); Section 4 characterizes lithium slag's mineralogical and chemical properties (e.g., the main components and phase composition) to lay a foundation for its resource utilization; Section 5 explores lithium slag's high-value utilization schemes, focusing on gypsum recovery, silica–alumina micro-powder preparation, and strategic metal recovery from fine tantalite concentrate slag; and Section 6 summarizes the key findings, identifies current utilization bottlenecks (e.g., technical/cost issues), and proposes prospects for efficient, large-scale lithium slag utilization.

2. Characteristics of Lithium Resources

2.1. Forms of Lithium

With the rapid development of mobile power sources and electric vehicles, the applications of lithium are increasing [14]. In recent decades, the supply–demand imbalance of lithium has become prominent, and its sources have gradually changed. According to Li Xiaoguang [15], the global lithium demand increased by 25% year-on-year in 2024, while supply only increased by 18%, expanding the supply–demand gap to 7%, directly driving the diversification of lithium resource development. These sources are mainly categorized into the following: brine-type lithium resources, which can be further divided into salt-lake brine (58%) and deep brine (6%) [16]; hard-rock-type resources [17], which can be subdivided into spodumene ($LiAl(SiO_3)_2$) granite and granite types, accounting for 26% of the global total; and clay-type resources, which are relatively rare, at about 10% [18].

Brine from salt lakes is the largest discovered source of lithium. Compared to other types of ore mining, lithium extraction from salt-lake brine has advantages such as better environmental performance and lower costs, making it one of the main types of lithium deposits being developed in the world today [19]. However, the global distribution of salt-lake brine lithium resources is highly concentrated—approximately 70% of the world's reserves are concentrated in the Andean "Lithium Triangle", which encompasses Salar de Atacama (Chile), Salar de Olaroz (Argentina), and Salar de Uyuni (Bolivia) [20]. This high geographical concentration exposes the lithium supply chain to dual risks. Geopolitically, uncertainties such as Chile's lithium nationalization policies may undermine stable access to lithium resources [21]. Technically, solar evaporation, the primary process for salt-lake lithium extraction, requires a long cycle of 6–12 months and is highly dependent on arid environmental conditions [22]. Notably, seasonal rainfall variations in arid regions can directly compromise the continuity and efficiency of production.

Chinese salt lakes are renowned for their large number, diverse types, abundant resources, and high content of rare elements [23]. However, most of these salt-lake brine resources in China exhibit a relatively high Mg^{2+}/Li^+ ratio. As presented in Table 1. the Qarhan Salt Lake [24] has a Mg^{2+} concentration of 108.5 g/L versus a Li^+ concentration of 3.279 g/L. This elevated ratio necessitates additional Mg^{2+}–Li^+ separation steps, such as ion-sieve adsorption and solvent extraction, which increases process complexity and operational costs, ultimately offsetting the inherent low-cost advantage of brine-based lithium extraction. The water chemistry properties of salt lakes are key factors in salt-lake lithium extraction technology processes. Ion concentrations in salt lakes serve as the basis for the classification of salt-lake water chemistry types, including Li^+, Mg^{2+}, K^+, Na^+, Ca^{2+}, SO_4^{2-}, etc. Table 1 shows the composition of brine resources in the world's major salt lakes. These compositional differences directly dictate the selection of lithium extraction processes: the Salar de Atacama [25] (with a low Mg^{2+}/Li^+ ratio of 5.8:1) can adopt a simple process, combining solar evaporation and carbonate precipitation, while the Qarhan Salt Lake [24] (with a high Mg^{2+}/Li^+ ratio of 33.1:1) requires the pre-separation of magnesium, resulting in significant disparities in production costs.

Table 1. Compositions of the main global salt-lake brine resources (g/L) (Reproduced with permission from [26], published by Springer Nature Switzerland AG, 2023).

Salt-Lake Brine	Li^+	Mg^{2+}	K^+	Na^+	Ca^{2+}	SO_4^{2-}
Qarhan Salt Lake, China [24]	3.279	108.5	0.763	2.281	0.107	6.39
Atacama Salar Brine, Chile [25]	3.02	17.6	28.2	61.9	0.41	37.9
Olaroz Salar Brine, Argentina [27]	1.01	2.00	6.22	98.85	0.51	10.07
Uyuni Salar Brine, Bolivia [28]	0.57	13.3	14.2	53.1	0.48	0.48

Table 1. *Cont.*

Salt-Lake Brine	Li^+	Mg^{2+}	K^+	Na^+	Ca^{2+}	SO_4^{2-}
Yiliping Salt Lake, China [29]	0.33	26.29	15.11	78.02	-	25.50
Longmucuo Salt Lake, China [30]	0.865	75.41	15.59	11.10	0.12	25.9
West Taijinar Salt Lake, China [31]	0.784	60.58	16.00	21.01	0.185	25.08
East Taijinar Salt Lake, China [32]	6.75	85.47	7.69	10.42	-	29.58
Zabuye Salt Lake, China [33]	0.16	21.4	7.10	69.2		40.5

Hard-rock lithium ores mainly include spodumene ($LiAl(SiO_3)_2$), lepidolite ($K(LiAl)_3[AlSi_4O_{10}](OHF)_2$), and iron-bearing lepidolite [34–36]. The largest lithium ore reserves are currently found in spodumene ($LiAl(SiO_3)_2$) and lepidolite, which are the main sources of lithium extraction. Spodumene ($LiAl(SiO_3)_2$), as the primary raw material for lithium extraction, has a simple mineral composition and a high lithium grade, with a Li_2O content of approximately 2.9% to 7.7% [37]. Figure 1 [35] illustrates the key morphological and microstructural characteristics of spodumene ($LiAl(SiO_3)_2$). Specifically, Figure 1a presents the macroscopic (optical) appearance of typical α-spodumene, which exhibits a prismatic crystal habit and distinct cleavage planes—features that serve as diagnostic criteria for its preliminary identification in ore samples. Figure 1b displays its microscopic morphology via scanning electron microscopy (SEM), revealing a relatively dense, blocky particle structure. In contrast, Figure 1c,d depict the macroscopic and microscopic characteristics of β-spodumene, respectively. The phase transformation from α-spodumene to β-spodumene, induced by high-temperature roasting (as detailed in Section 3, is characterized by the formation of reddish-brown particles (Figure 1d) and a more porous microstructure compared to α-spodumene. Notably, the SEM mapping analysis shown in Figure 1 further illustrates the distribution of lithium in spodumene. In α-spodumene (Figure 1a,b), lithium is uniformly distributed within the crystalline lattice, indicating its stable incorporation into the $LiAl(SiO_3)_2$ structure; in β-spodumene (Figure 1c,d), the phase transition causes slight variations in lithium distribution, with localized enrichment observed in the reddish-brown particle regions (Figure 1d). This phenomenon is closely associated with the enhanced reactivity of β-spodumene in subsequent lithium extraction processes (e.g., acid leaching or alkali decomposition). Lepidolite has a complex composition, with a lower lithium grade than spodumene ($LiAl(SiO_3)_2$), and its Li_2O content is approximately 2.0% to 5.0% [38]. The biggest difference between lepidolite and spodumene ($LiAl(SiO_3)_2$) is that lepidolite contains 5.9% fluorine [39]. The study of lithium resources extracted from lithium ores is of great significance to the development of China's lithium industry.

Clay-type lithium resources are sedimentary and are usually classified as volcanic clastic weathered, silico-aluminous, and coal-bearing clay subtypes [40]. Due to the small proportion of clay-type lithium resources, directly extracting lithium without pre-concentration presents issues, which include high reagent consumption, which refers to the large quantities of leaching agents (sulfuric acid or composite acid systems) required to react with the scattered lithium-bearing minerals in low-grade ores; high energy consumption, which mainly comes from two aspects: prolonged heating during leaching—since lithium in clay minerals has low accessibility, extended thermal maintenance is needed to promote the interaction between reagents and lithium—and additional energy for ore grinding, which reduces the particle size of ores to enhance their reactivity; and environmental pollution, which stems from the discharge of unreacted acidic leaching agents and heavy metal-containing wastewater, as clay ores often contain associated heavy metals such as iron and manganese that are leached alongside lithium and can contaminate water bodies if untreated. In recent years, several large clay lithium mines have been discovered in regions

such as Yunnan, Inner Mongolia, and Qinghai in China, and with the enormous demand for lithium, clay-type resources are receiving increasing attention [41].

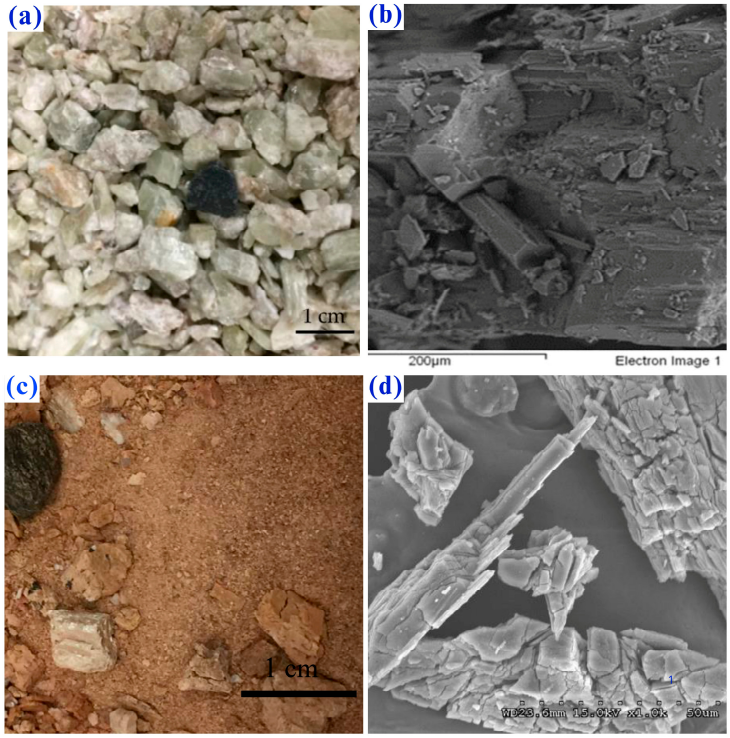


Figure 1. (**a**) Macroscopic (optical) and (**b**) microscopic (SEM) aspects of a typical α-spodumene sample; (**c**) macroscopic (optical) and (**d**) microscopic (SEM) aspects of a typical β-spodumene sample (red-brown particles) [35].

2.2. The Distribution of Spodumene Ore

According to data from the 2024 United States Geological Survey (USGS) report [42], global lithium resources are estimated to be around 105 million tons, with proven lithium reserves of 28 million tons. The global distribution of lithium reserves is highly concentrated, mainly in the Americas and Australia. The major lithium resource-rich countries include Chile, Australia, Argentina, and China. The relevant data are shown in Figure 2.

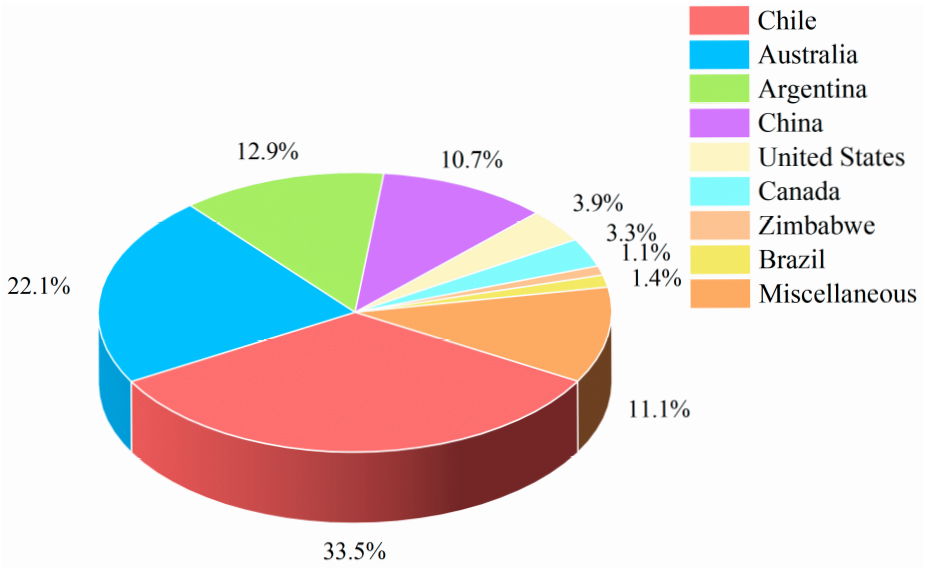


Figure 2. Global lithium resource distribution map [42].

The global distribution of lithium resources is extensive. Based on geographical location and formation conditions, its deposits can be classified into three major types: hard-rock lithium, brine lithium, and clay lithium. These three types can be further subdivided into seven genetic types, and Table 2 shows details on their research and exploitation degrees, as well as typical deposits. The distribution of brine lithium resources is highly uneven globally. However, China is rich in salt-lake lithium resources, which can be mainly divided into four regions: the Tibetan Plateau Salt-lake District, the Northwest Salt-lake District, the Northeast Salt-lake District, and the scattered salt lake districts in eastern areas [43]. The Tibetan Plateau is the largest producer of brine-type lithium deposits in China, with Qinghai and Tibet accounting for approximately 80% of the country's lithium resources [44].

Table 2. Classification of the world's primary lithium resources [44–48].

Genetic Type	Research and Exploitation Degrees	Typical Deposits
Salt-lake brine type	High degree of research and exploitation	Altiplano Lithium Triangle (Andes, South America), salt lakes on China's Qinghai–Tibet Plateau, salt lakes in the southwestern U.S.
Deep brine type	Great potential, but a low degree of research	Cenozoic tectonic zone in the western Qaidam Basin, China; deep Triassic brine in Huangjinkou, Xuanhan, Sichuan Basin, China
Granite pegmatite type	High grades and extensively surveyed	Greenbushes lithium deposit (Australia), Altay deposit (Xinjiang, China), Jiajika and Maerkang deposits (Sichuan, China)
Granite type	Low grades, high exploitation costs	Brazilian granite lithium deposits
Pyroclastic weathered clay subtype	Formed by weathering and lithium enrichment of lithium-bearing pyroclastic rocks	Kings Valley (Nevada, U.S.), a valley in the south-central Mexican Plateau
Silico-aluminous clay type	Formed in the Neopaleozoic, widely distributed	Dazhuyuan deposit (Guizhou, China)
Coal-measure clay type	Widely distributed, low exploration degree	Jungar coal field (China), Ningwu coal field (Shanxi Province, China)

In terms of hard-rock lithium resources, they are mainly distributed [49] in Sichuan, Jiangxi, Xinjiang, Hunan, and other regions of China: spodumene ($LiAl(SiO_3)_2$) deposits are concentrated in the Garzê and Aba areas of Sichuan; lepidolite deposits are widely distributed in Jiangxi; Xinjiang is dominated by granite pegmatite-type hard-rock resources (once a major lithium mineral resource province); and Hunan also holds a certain proportion of the country's total lithium reserves [50–52]. Overall, China's lithium resources are unevenly distributed, but different regions have their own advantages in resource types, providing a diversified foundation for the development and utilization of China's lithium resources [53].

3. The Main Source of Lithium Slag

The traditional processes for extracting lithium from spodumene ($LiAl(SiO_3)_2$) include the acid process, alkali process, salt roasting process, and chlorination process. As shown in Figure 3, the traditional process of extracting lithium from spodumene ($LiAl(SiO_3)_2$) mainly includes the following steps: First, it is converted into β-spodumene through the high-temperature roasting of α-spodumene. The insoluble lithium compounds are then

converted into soluble lithium compounds under high pressure using an acid or alkaline solution. Finally, lithium carbonate is obtained via carbonate precipitation [54].



Figure 3. The conventional extraction process of lithium from spodumene ($LiAl(SiO_3)_2$) (Reproduced with permission from [54,55], published by Elsevier). Note: The figure illustrates the workflow of the acid and alkali processes, showing the complete path from α-spodumene to lithium carbonate, including the generation of lithium slag as a by-product.

3.1. Acid Process

The sulfuric acid method, invented in 1943, is the main process for extracting lithium from spodumene ($LiAl(SiO_3)_2$) and lepidolite ($K(LiAl)_3[AlSi_4O_{10}](OHF)_2$). α-spodumene (monoclinic structure, density 3.184 $g{\cdot}cm^{-3}$) [56] exhibits high acid inertness due to its dense crystalline lattice that restricts Li^+ accessibility, while β-spodumene (tetragonal structure, density 2.374 $g{\cdot}cm^{-3}$) [57] has a porous microstructure with pseudo-zeolitic channels, enabling efficient ion exchange with acids. Around 1000 °C, α-spodumene undergoes a phase transformation (accompanied by ~27% lattice expansion) to form β-spodumene [58]. This transformation is driven by a high-temperature-induced lattice rearrangement, which breaks the compact Li-Al-Si-O framework of α-spodumene and converts it into a more reactive structure [59]. The reaction between spodumene ($LiAl(SiO_3)_2$) and sulfuric acid follows the following equation [60]:

$$2LiAlSi_2O_{6(s)} + H_2SO_{4(l)} \overset{175\ ^\circ C}{\rightarrow} 2HAlSi_2O_{6(s)} + Li_2SO_{4(s)} \quad (1)$$

$$Li_2O \cdot Al_2O_3 \cdot 4SiO_{2(s)} + H_2SO_{4(l)} \overset{175\ ^\circ C}{\rightarrow} Li_2SO_{4(s)} + Al_2O_3 \cdot 4SiO_2 \cdot H_2O_{(S)} \quad (2)$$

In Equation (3), the Li^+ from spodumene ($LiAl(SiO_3)_2$) is replaced with H^+ from the acid, leaving the framework unchanged. Excess acid will then react with the formed Li_2SO_4 to produce $LiHSO_4$ (melting point of ~170 °C), which exists in a liquid state and prolongs the acid–spodumene reaction:

$$Li_2SO_{4(s)} + H_2SO_{4(l)} \rightarrow 2LiHSO_{4(l)} \quad (3)$$

Proven through the practices of many companies (e.g., operations at Greenbushes mine, Australia), the overall yield of this process is above 96%. The sulfuric acid method has a wide range of applications and can handle spodumene ($LiAl(SiO_3)_2$) of different grades. However, there are still some issues that restrict its development. First, the acid consumption of the production process is high (30%–140% excess acid is required to neutralize impurities such as K^+ and Na^+). Second, a large amount of silico-aluminous

lithium slag (containing ~60%–70% SiO_2 and 15%–20% Al_2O_3) is generated. Moreover, after leaching with sulfuric acid, limestone is needed for neutralization, resulting in a large amount of calcium sulfate.

In response to the issues of high sulfuric acid consumption and significant energy expenditure during the sulfuric acid roasting process, many researchers have compared the application of microwave ovens in the acid roasting process for lithium extraction from spodumene ($LiAl(SiO_3)_2$) with traditional furnaces. Salakjani et al. [60] found that the conventional acid roasting of 5 g of β-spodumene for 60 min at 250 °C in the presence of 80% excess concentrated sulfuric acid was highly effective for lithium extraction, and the microwave process achieved the almost complete recovery of lithium after 20 s of irradiation (Figure 4). Rezaee et al. [61] found that an optimal lithium recovery rate of 97% could be achieved using the microwave roasting–acid leaching process at a microwave power of 2.0 kW, which is comparable to the conventional heating process. Importantly, microwave heating has the advantages of fast calcination speed, low energy consumption, and no greenhouse gas emissions. While the studies by Salakjani and Rezaee have demonstrated the potential of microwave-assisted technology in spodumene lithium extraction, they still suffer from limitations that hinder industrial scalability, such as reliance on small-scale experiments, excessive residual sulfuric acid, and high upfront costs. To address the long-standing "high acid consumption and high energy consumption" bottlenecks of the traditional sulfuric acid process, Tian et al. [62] proposed an integrated "microwave-induced phase transformation + microwave acid roasting + mechanical ball milling leaching" scheme. This innovative approach delivers notable improvements: the microwave-assisted phase transformation temperature of α-spodumene is reduced to 900 °C (down from 1050 °C in conventional processes), with the transformation time shortened to 30 min; the sulfuric acid dosage is cut to 1.2 times the theoretical requirement (compared to 1.5–2.0 times in traditional methods), reducing waste slag production by 20%; and mechanical ball milling enhances the leaching efficiency, enabling a stable lithium recovery rate of over 96%.

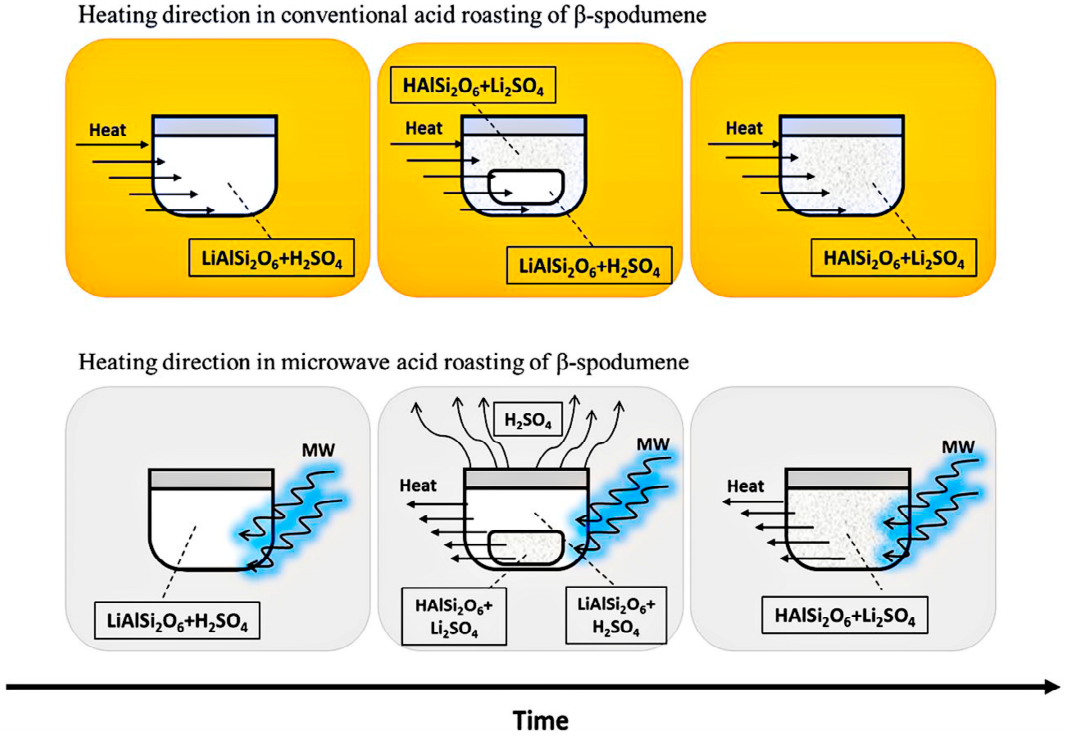


Figure 4. Comparison of the heating direction of spodumene in conventional acid-solution roasting and microwave processes (Reproduced with permission from [60], published by Elsevier Ltd., 2019).

A study by Zhou et al. [63] found that a mixed solution of H_2SO_4 and $FeCl_3$ has a synergistic effect. When combined, they can be used to extract lithium from clay-type lithium ores. The highest lithium leaching efficiency is achieved at 600 °C. After calcination at 600 °C for 60 min, using a mixture of 10.5 wt.% H_2SO_4 and 2 wt.% $FeCl_3$ with a liquid-to-solid ratio of 5 mL/g, and leaching at 80 °C for 90 min, the lithium leaching rate can reach as high as 96.18%—notably higher than the ~73% lithium recovery from bauxitic clay via single sulfuric acid leaching, as reported by Gu et al. [64], underscoring the synergistic enhancement of $FeCl_3$. XRD and SEM results indicate that lithium extraction is an ion-exchange process (Figure 5). As shown in the red box of Figure 5, it can be observed that the layered silicate structure of the calcined clay minerals is destroyed during the leaching process, while crystal aggregation occurs after the leaching process. The synergistic effect of H_2SO_4 and $FeCl_3$ is attributed to Fe^{3+} entering the interlayer of the clay mineral's layered structure. This not only releases Li^+ but also increases the interlayer spacing, facilitating the entry of H^+ into the interlayer and thereby promoting the exchange between H^+ and Li^+. Moreover, the mixed solution of H_2SO_4 and $FeCl_3$ also has the advantages of a short reaction time, low acidity, and low energy consumption. It reduces acid dosage while maintaining high efficiency.

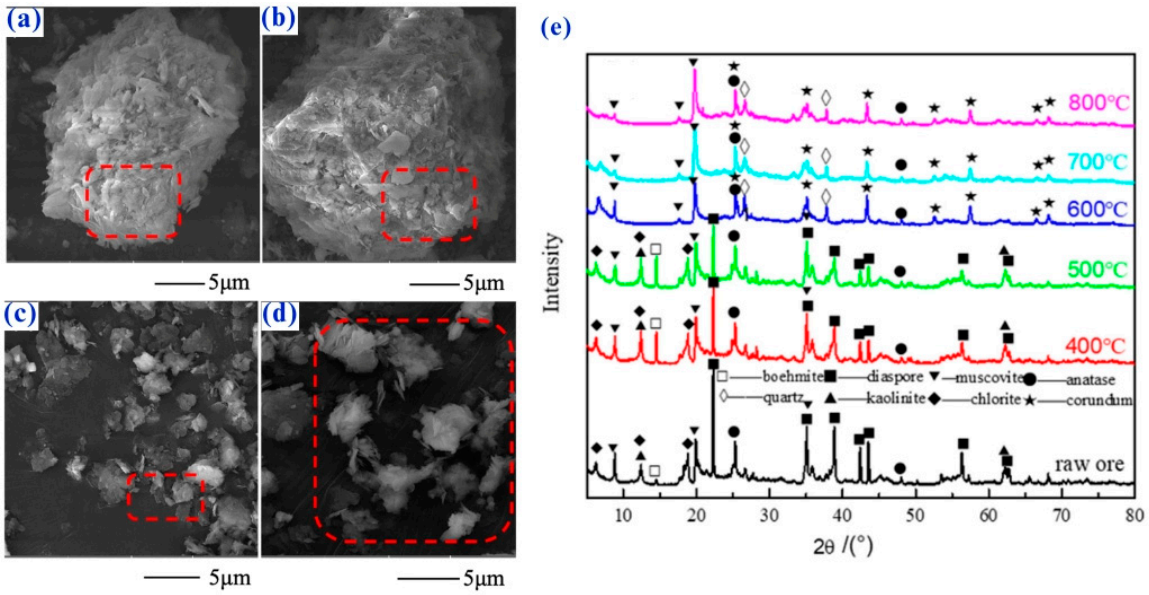


Figure 5. SEM images of (**a**) the raw ore, (**b**,**c**) the calcined ore at 600 °C, (**d**) leaching residue obtained under optimal conditions, and (**e**) the XRD results of the raw ore and products obtained after the calcination process [63].

Paris et al. [65] selected phosphoric acid as the leaching agent for lithium extraction. They conducted experiments on 1 g of pure β-spodumene, and during the roasting process, ion exchange occurred between the protons of the phosphoric acid and the lithium ions of the spodumene, forming soluble lithium phosphate according to Equation (4):

$$Li_2O \cdot Al_2O_3 \cdot 4SiO_{2(s)} + 2H_3PO_{4(l)} \overset{100\ ^\circ C}{\rightarrow} 2Li_3PO_{4(l)} + Al_2O_3 \cdot 4SiO_2 \cdot 3H_2O_{(S)} \quad (4)$$

By varying the concentration of phosphoric acid, temperature, residence time, and liquid-to-solid ratio, they found that a maximum lithium extraction rate of 48% was achieved under the conditions of an 8 M acid concentration, 100 °C temperature, 24 h retention time, and liquid-to-solid ratio of 10 mL/g. To maintain a lithium extraction rate greater than 40%, the minimum retention time required is 8 h. With further improvements

and an understanding of the leaching mechanism, phosphoric acid may prove to be a suitable alternative for selective lithium extraction from spodumene.

To tackle the large-scale production of aluminosilicate lithium slag in lithium extraction, Zhang et al. [66] developed a technology for the efficient recovery of lithium from spodumene acid clinker, as well as the co-production of a low-iron, low-sulfur silica-alumina micro-powder. The process is as follows. First, the spodumene acid clinker is leached with water to form a slurry, which is separated into leaching residue 1 and filtrate 1. Second, leaching residue 1 is stirred and washed with water to generate a washing slurry, yielding filtrate 2 and washing residue 1 after separation. Finally, washing residue 1 is mixed with water for grinding and classification to obtain a fine-grained slurry, which is further processed into the target micro-powder. This method eliminates the risk of over-standard sulfur in the final products caused by the gradual accumulation of lithium salts in recycled water and supports the subsequent recycling of the lithium slag.

3.2. Alkali Method

The main method for producing LiOH in the 1970s and 1980s was limestone roasting, which was the earliest method for extracting lithium from spodumene [67]. Spodumene is mixed with lime or limestone in a certain proportion and then subjected to roasting, leaching, washing, leachate concentration, and purification to obtain a high-concentration lithium-containing solution. However, the limestone roasting process has a large amount of slag, high energy consumption, a low lithium leaching rate, and the resulting lithium salt has low purity.

In the practice of extracting lithium from spodumene, the traditional limestone roasting process struggles to meet the requirements of efficient production due to its large slag output and high energy consumption. Against this backdrop, the sodium carbonate pressure leaching method, leveraging its significant advantages, has now been widely promoted and applied. This method mainly comprises four major processes: crystalline phase transformation, roasting, pressure leaching, carbonation dissolution, and lithium precipitation. Through roasting, the refractory natural α-spodumene is transformed into more readily processable β-spodumene. In the presence of liquid water and at elevated temperature and pressure, sodium carbonate reacts with β-spodumene to facilitate a displacement reaction between sodium and lithium.

Taking α-spodumene from Xinjiang (containing 6.05% Li_2O and 60.31% SiO_2) as the raw material, Chen et al. [68] first calcined it at 1050 °C to convert it into β-spodumene, then treated the β-spodumene using the sodium carbonate autoclave process and optimized the process parameters. The results showed that when steel balls were added for stirring (stirring speed of 300 r/min), the liquid-to-solid ratio was 4, and the reaction was carried out at 225 °C for 60 min, the lithium extraction rate exceeded 96%, which was equivalent to that of the sulfuric acid method, while avoiding the drawbacks of the latter. The "roasting–autoclave–carbonization separation" process proposed by Chen et al. [68] not only retains the inherent advantages of the sodium carbonate autoclave method, such as a short process flow and low equipment corrosion, but also eliminates the insufficient lithium leaching rate through process parameter optimization (with a lithium extraction rate exceeding 96%), providing support for the industrialization of this process. However, the study fails to analyze the environmental and economic indicators of the process, such as the recycling rate of sodium carbonate, as well as the consumption and emission of CO_2 during the carbonization stage. These indicators are important considerations for the industrial implementation of the process, limiting the industrial guiding value of the research conclusions.

In Tian's research [69] on lithium extraction using the soda ash pressure leaching method, single-factor experiments were conducted to investigate the effects of the sodium-to-lithium ratio, liquid-to-solid ratio, temperature, time, and stirring rate on the conversion rate. Firstly, lithium was extracted in the form of lithium carbonate, with the following reaction equation:

$$Li_2O \cdot Al_2O_3 \cdot 4SiO_{2(s)} + nH_2O + Na_2CO_3 \rightarrow Na_2O \cdot Al_2O_3 \cdot 4SiO_2 \cdot nH_2O + Li_2CO_3 \quad (5)$$

The process then proceeds to carbonate leaching, which primarily relies on the gas–liquid–solid three-phase reaction between CO_2 and slightly soluble Li_2CO_3 in an aqueous solution to form the more soluble $LiHCO_3$. The overall reaction equation is as follows:

$$Li_2CO_3 + CO_2 + H_2O \rightarrow 2LiHCO_3 \quad (6)$$

Through carbonation leaching, lithium is separated from most impurities and exists in the leachate in the form of $LiHCO_3$. The filtrate is heated at a constant temperature and then filtered while still hot. Finally, lithium carbonate crystals are obtained by drying. The reaction equation is as follows:

$$2LiHCO_3 \rightarrow Li_2CO_3 + CO_2 + H_2O \quad (7)$$

The study found that a lithium extraction rate of 96% could be achieved with a sodium-to-lithium ratio of 1.25, a liquid-to-solid ratio of 4, and a stirring rate of 300 r/min. Tian Qianqiu's research provides a solid foundation for the soda ash pressure leaching method, clarifying key parameters and mechanisms that advance the technology beyond theoretical exploration.

Subasinghe and Rezaee [70] proposed a "NaOH low-temperature roasting-water leaching" direct lithium extraction technology to solve the high energy consumption and pollution of traditional α-spodumene lithium extraction. Using an α-spodumene concentrate (93 ± 1.5% α-spodumene, ~6% Li_2O) as the raw material, they determined single-stage optimal conditions via single-factor experiments: a 1.5:1 NaOH-to-ore mass ratio, roasting at 325 °C for 2 h (converting α-spodumene to water-soluble Li_3NaSiO_4), and room-temperature water leaching (10% solid–liquid ratio, 100 rpm stirring), achieving a 77 ± 3.4% lithium leaching rate. To address the mass transfer obstruction of the sodium aluminosilicate product layer, a two-stage process was designed: second-stage roasting (1:1 NaOH-to-first-stage-residue ratio, 325 °C for 10 min) followed by water leaching (1% solid–liquid ratio, 200 rpm), resulting in total lithium recovery of over 99%, which is superior to the traditional sulfuric acid method (~96%). Mechanistically, roasting follows the "shrinking core model". Water leaching is a spontaneous exothermic reaction ($\Delta H < 0$) with NaOH regeneration (leachate pH ≈ 13), reducing downstream reagent consumption; however, the process lacks verification for low-grade spodumene adaptability and continuous industrial application.

3.3. Salt Roasting Method

In the spodumene salt roasting method, the most commonly used salt is potassium sulfate. Spodumene will change from α-spodumene to β-spodumene at high temperatures [71], and then potassium sulfate is added to generate soluble potassium sulfate. A lithium-containing solution is obtained after water leaching, and then impurities are removed and sodium carbonate is precipitated to generate lithium carbonate (Figure 6). Compared with the acid method, the sulfate method can reduce the dissolution of Al and Fe, simplifying the subsequent purification process and thereby reducing the loss of lithium.

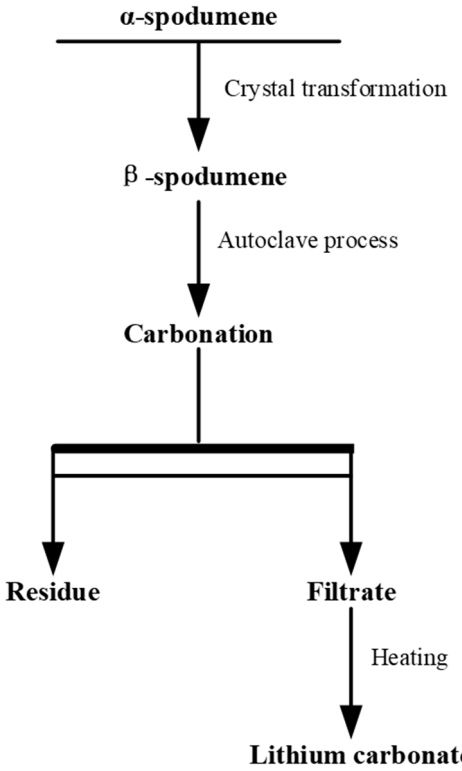


Figure 6. Flowchart for the preparation of lithium carbonate.

Liu et al. [72] developed an innovative method for producing a lithium sulfate solution by using the sulfate roasting process on spodumene. The method comprises the following steps. First, spodumene ore is uniformly mixed with roasting additives at a specific ratio, then the mixture is placed in a muffle furnace for roasting, obtaining a roasted product. After cooling the roasted product, it is leached with water to yield a lithium sulfate solution. This spodumene sulfate roasting method for lithium sulfate solution production consists of two core processes: roasting and water leaching. Notably, the roasting temperature is lower than the phase transition temperature required for traditional high-temperature calcination, and the water leaching step eliminates the need for acid leaching, thereby avoiding issues such as equipment corrosion caused by acid. This not only reduces energy consumption but also enhances the economic efficiency of producing the lithium sulfate solution from spodumene.

Samoilov et al. [73] analyzed the technical potential of the sulfate roasting method from an international perspective, highlighting its unique advantage in processing high-aluminum spodumene (with an Al_2O_3 content > 25%). During the roasting process, aluminum can react with sulfate to form stable aluminum sulfate complexes, which remain in the solid phase and do not dissolve into the leachate—this effectively solves the problem of a high level of aluminum impurities in the leachate, which plagues other processes. For instance, when using $FeSO_4$ as the roasting additive, roasting at 675 °C for 1.5 h not only achieves a lithium leaching rate of 92.7% but also enables the simultaneous recovery of associated rare metals, such as rubidium (87.1%) and cesium (82.6%), significantly enhancing the comprehensive utilization value of spodumene ore. However, the literature also points out that the core challenge of this method lies in the recovery and recycling of sulfate additives. Currently, only about 60% of unreacted sulfate can be recovered in industrial applications; the remaining portion is lost along with leaching residues, which directly leads to high reagent costs and reduces the economic viability of the process. To address this issue, future research should focus on process optimization.

Chen et al. [74] proposed a salt gypsum-assisted sulfate method for extracting lithium from spodumene, with the following process flow and advantages. First, pre-treatment is carried out, where spodumene is crushed to obtain a powder. During mixing, composite sulfate, salt gypsum, an anti-caking agent, and absolute ethanol are added, and the mixture is prepared through the process of "holding at 90–100 °C for 1–2 h → holding at −10~−5 °C for 3–5 h". The mixture is mixed with modified calcium oxide, calcined at 900–1000 °C for 60–70 min, cooled, and ground to obtain the calcined material. Then, the calcined material is soaked in 0.4–0.6 mol/L dilute sulfuric acid for 50–70 min to leach the lithium. Finally, lithium carbonate is obtained through lithium precipitation. This method utilizes the synergistic effect of salt gypsum and auxiliaries, which reduces costs, improves the lithium leaching rate and the purity of lithium carbonate, solves the pain points of traditional processes, and has industrial application potential.

Chen et al. [75] proposed a method for producing lithium carbonate from spodumene using a sodium carbonate autoclaving process. They also investigated various operating conditions, including the liquid-to-solid ratio, Na/Li ratio, stirring speed, reaction temperature, and reaction time, to evaluate their effects on the carbonate conversion efficiency. Their results indicated that when the liquid-to-solid ratio was 4, the Na/Li ratio was 1.25, the stirring speed was 300 revolutions per minute, the reaction temperature was 225 °C, and the reaction time was 90 min, the carbonate conversion efficiency was no less than 94%. The purity of the obtained lithium carbonate could reach 99.6%. Details regarding how each operating condition influences carbonate conversion efficiency, as well as the XRD pattern of residues processed using the chlorination method, are presented in Figure 7.

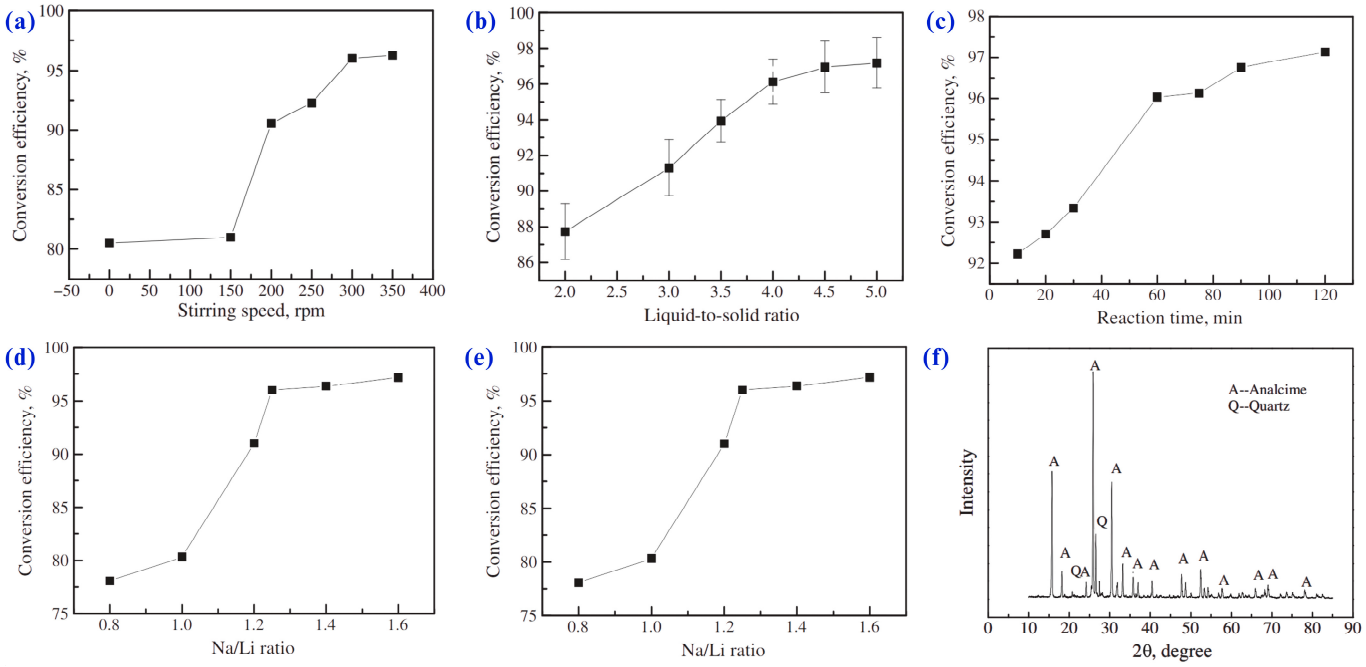


Figure 7. The impact of various factors on the conversion efficiency of lithium carbonate: (**a**) liquid-to-solid ratio; (**b**) Na/Li; (**c**) stirring speed; (**d**) reaction temperature; (**e**) reaction time; (**f**) XRD pattern, using the chlorination method on the residue (Reproduced with permission from [75], published by Elsevier B.V., 2011).

3.4. Chlorination Method

The chlorination roasting method is similar to the spodumene sulfuric acid method, both of which first convert α-spodumene into β-spodumene at high temperatures. Then, at 900 °C, β-spodumene will be roasted with chlorine at a high temperature to extract lithium chloride.

Barbosa et al. [76] investigated the recovery of lithium from spodumene using pure chlorine gas and compared EM micrographs of the residual samples obtained from chlorination at 1000 °C, 1050 °C, and 1100 °C (Figure 8). They found that at 1100 °C, β-spodumene was roasted using pure chlorine gas and extracted as lithium chloride for 150 min, with silicon and aluminum not being chlorinated but remaining in the form of solid secondary residues in the form of $Al_6Si_2O_{13}$ (mullite) and Si_2O (cristobalite).

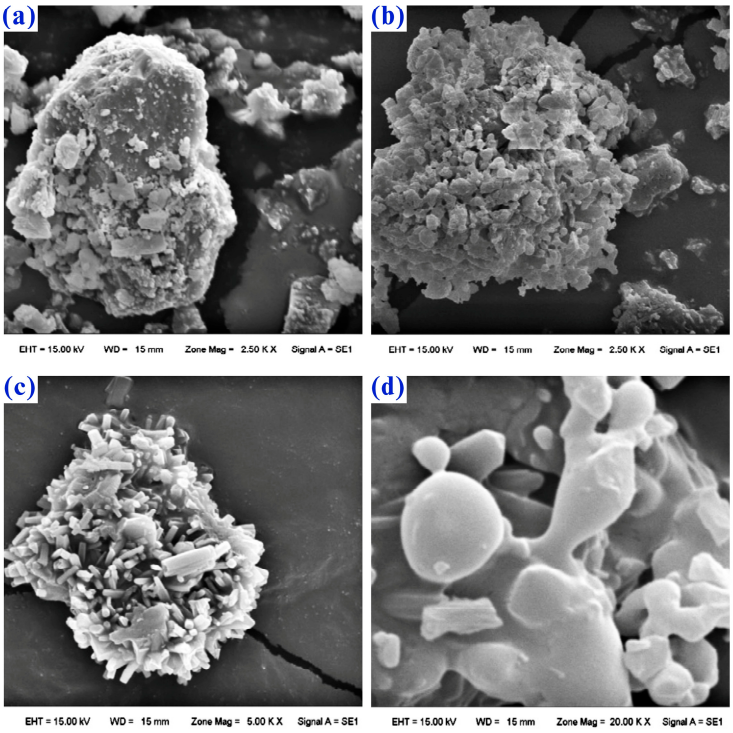


Figure 8. SEM micrographs of the residual samples obtained from chlorination at (**a**) 1000 °C, (**b**) 1050 °C, and (**c**,**d**) 1100 °C (Reproduced with permission from [76], published by Elsevier B.V., 2014).

He [77] and his team have proposed a new method for lithium extraction from spodumene, with the specific process route as follows. First, the raw spodumene ore is crushed, then mixed with chlorination roasting aids such as calcium chloride and magnesium chloride and subjected to ball milling to prepare the activated materials. Next, chlorination roasting is carried out on these activated materials, and finally, the chlorination roasting products are treated with water leaching to obtain a lithium chloride solution. The core advantage of this method is that, by virtue of the synergistic effect of mechanical activation, the raw spodumene ore forms metastable phases and amorphous phases. This not only significantly reduces the temperature required for subsequent chlorination roasting but also greatly improves the roasting efficiency, thus enabling the efficient extraction of lithium from spodumene at a relatively low temperature. This technological innovation has effectively addressed the existing problems in current spodumene lithium extraction processes, such as a high transformation temperature and low lithium extraction efficiency, and provided a more feasible solution for the efficient development and utilization of spodumene resources.

Braga et al. [78] investigated a chlorination roasting method for extracting lithium from Brazilian α-spodumene. Initially, the ore was pre-treated with calcium chloride and magnesium chloride, followed by leaching with water at 90 °C. Based on the model established using HSC version 5.1 software, as shown in Figure 9, the reaction products between spodumene and chlorides ($MgCl_2$:$CaCl_2$) were determined to be lithium chloride

(LiCl), calcium–magnesium silicate ($CaO{\cdot}MgO{\cdot}SiO_2$), magnesium aluminate ($MgO{\cdot}Al_2O_3$), and silicon dioxide ($SiO_2$). Supplementary experiments demonstrated that when the mass ratio of spodumene to chlorides was 1:6, the molar ratio of $MgCl_2$ to $CaCl_2$ was 2:1, the roasting temperature was 1150 °C, and the roasting time was 30 min, the lithium extraction efficiency could reach above 95%, as shown in Figure 9.

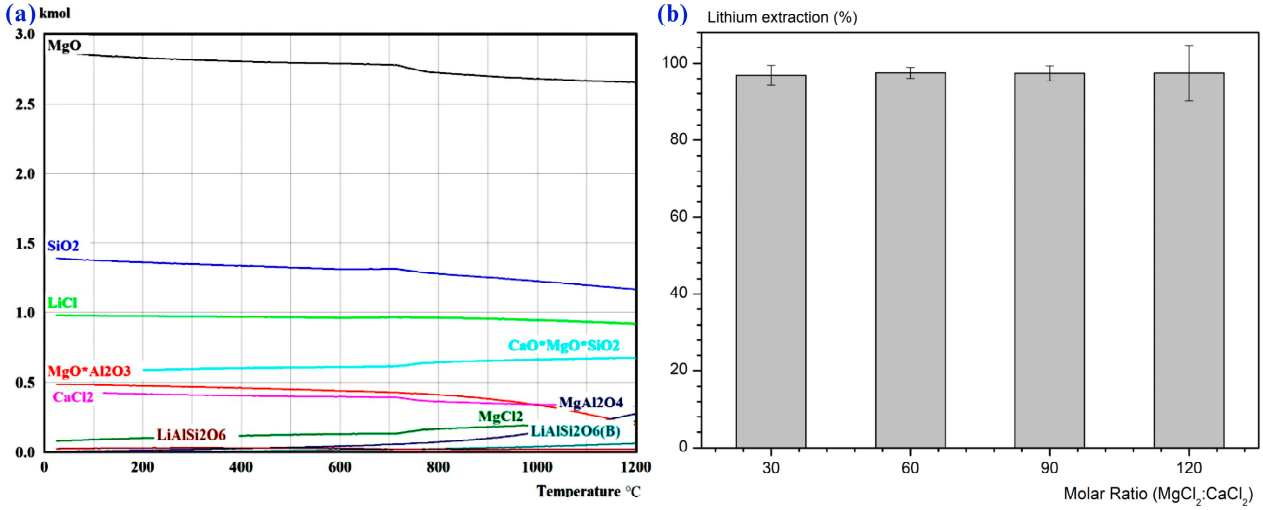


Figure 9. (**a**) HSC model of the α-spodumene/$MgCl^{2+}$ $CaCl_2$ mixture; (**b**) changes in lithium extraction (%) as a function of the chlorination roasting period [78]. Note: The '*' in the figure represents the composite oxide relationship, which is equivalent to '·'.

4. Chemical Composition and Mineralogical Characterization of Lithium Slag

4.1. Mineralogical Characterization of Lithium Slag

Lithium slag usually appears to be yellowish-gray or yellowish-white, with slight color variations depending on its origin. After drying, it becomes powdery, exhibits small particle sizes (generally 1–100 μm), and has a certain degree of adhesiveness. The particles of lithium slag are fine and have good grindability. Due to its porous structure with a large internal surface area (e.g., a specific surface area of ~10–30 m^2/g, as reported in related studies), it can be used to synthesize high-value-added products such as zeolite, the porous structure of which is key to zeolite synthesis, while its chemical composition later supports other applications such as auxiliary cementitious materials.

From a microscopic perspective, Wang et al. [79] further characterized the phase and composition of lithium slag by selecting lithium slag I, II, and III as analytical samples and observing them via back-scattered electron (BSE) microscopy, as shown in Figure 10 (BSE images of the three slags). The selected lithium slag I, II, and III are by-products generated after extracting lithium from spodumene (lithium pyroxene) via the sulfuric acid method, sodium carbonate pressure leaching method (alkali method), and potassium sulfate salt roasting method, respectively. Their formation processes correspond to the acid method, alkali method, and salt roasting process described in Section 3. Substances with a similar morphology and the same gray brightness (or color) are defined as belong to the same phase. There are also some amorphous phases in the lithium slag, which are mainly composed of Si, Al, and O elements according to energy dispersive X-ray spectroscopy (EDX) analysis. EDX analysis results of the three lithium slags are as follows: lithium slag I contains Si (45.2 wt.%), Al (18.7 wt.%), O (32.1 wt.%), and S (4.0 wt.%); lithium slag II contains Si (42.9 wt.%), Al (17.3 wt.%), O (34.5 wt.%), and S (5.3 wt.%); lithium slag III contains Si (46.5 wt.%), Al (19.2 wt.%), O (30.8 wt.%), and S (3.5 wt.%). Element mapping analysis further shows that SO_4^{2-} is mainly distributed in the gray-white granular

phase (corresponding to the gypsum phase), while Si and Al are uniformly distributed in the dark amorphous phase (corresponding to the silica-alumina phase). It was found that the SO_3 content in the three lithium slags was greater than 9%, in the form of SO_4^{2-}. Studying the content and state of SO_4^{2-} in lithium slag is conducive to its application as auxiliary cementitious materials (e.g., slag and fly ash), as the SO_4^{2-} content affects cementitious performance.

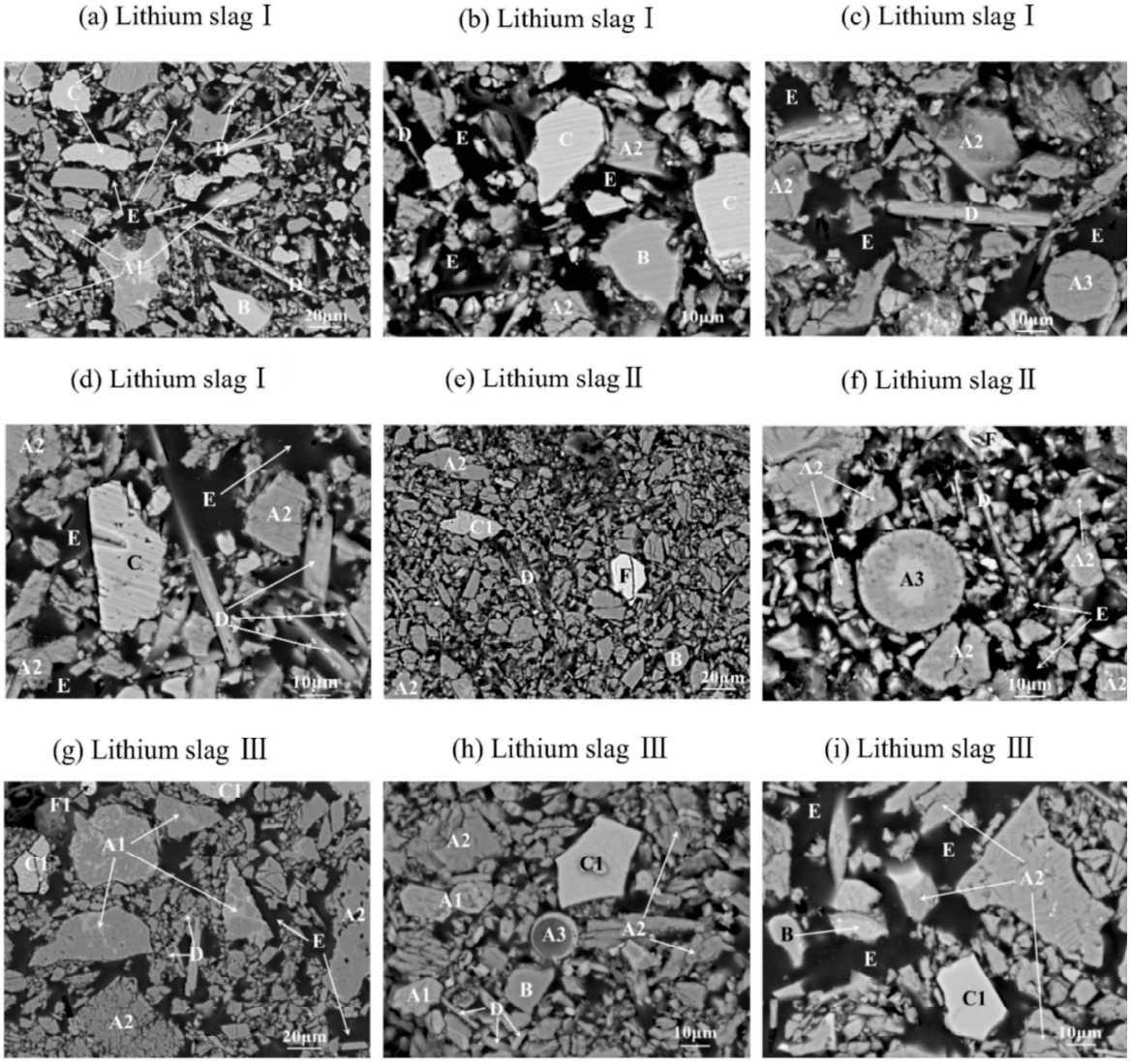


Figure 10. Back-scattered electron images of representative phases in lithium slag. Different letters (e.g., A1, A2, B, C, E, etc.) in the images indicate different phases or regions within the respective lithium slag samples. (The images are accompanied by EDX and element mapping analysis results: EDX data show the main elemental content of each slag (see text for details), and mapping results confirm the distribution of SO_4^{2-} in the gypsum phase and Si/Al in the silica-alumina phase) (Reproduced with permission from [79], published by Elsevier Ltd., 2019).

4.2. Chemical Composition of Lithium

Lithium slag is an industrial by-product of the process of extracting lithium from spodumene. It is produced through the high-temperature roasting of spodumene and sulfuric acid [80]. According to the production process, lithium slag is mainly divided into acid smelting and alkaline smelting. With the increasing demand for lithium resources year by year, lithium slag is piling up in large quantities. If it is not used, it will cause a significant level of pollution. Some scholars use XRD to study the phases of lithium slag, which mainly include the quartz phase (SiO_2), the gypsum phase ($CaSO_4 \cdot 2H_2O$), calcite

($CaCO_3$), pyrophyllite [$Al_2Si_4O_{10}(OH)_2$], and amorphous SiO_2 and Al_2O_3, as well as a small amount of spodumene ($LiAlSi_2O_6$), kaolinite, and lithium carbonate (Li_2CO_3). Qiu et al. [81] determined the chemical and mineralogical composition of slag via XPS and XRD measurements (Figure 11).

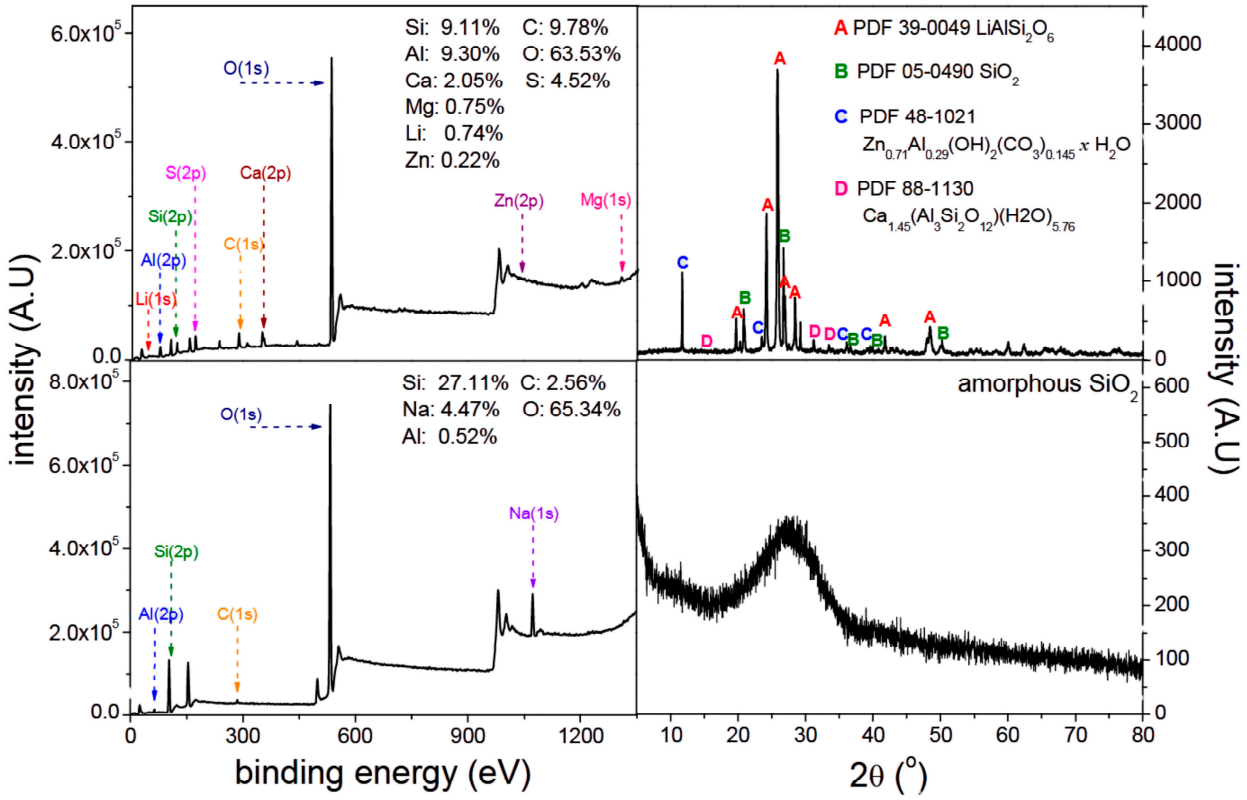


Figure 11. Survey scan XPS spectra and XRD patterns for pristine slag (Reproduced with permission from [81], published by RSC Publishing, 2016).

In addition, regarding the environmental risk assessment of lithium slag during storage and utilization, relevant studies (e.g., Li et al. [82]) have conducted toxic leaching tests on lithium slag generated by different processes. The results show that the leaching concentration of trace heavy metals (such as Fe and Mn, with contents usually <0.5 wt.%) in lithium slag is lower than the limit specified in identification standards for hazardous wastes and the identification of leaching toxicity, and no toxic elements (such as Pb and Cd) are detected. This indicates that lithium slag poses low environmental risks during reasonable storage or resource utilization.

The chemical composition of lithium slag is significantly affected by lithium extraction processes (such as the sulfuric acid method, alkali method, and salt roasting method). Lithium slags produced by different processes vary in the content of their main components, the types of impurities, and the occurrence states of valuable metals. These differences directly determine the direction of the resource utilization of the lithium slag. To clearly present the chemical composition characteristics of lithium slags from different processes, especially the content ranges of key components (e.g., SiO_2 and Al_2O_3), characteristic impurities (e.g., SO_3), and valuable rare metals (tantalum and niobium), Table 3 systematically compiles the typical data obtained from backscattered electron (BSE) microscopy, energy dispersive X-ray spectroscopy (EDX), and experimental tests in the reference document, providing a compositional basis for the targeted utilization of lithium slag.

Table 3. Typical chemical composition of lithium slags (by weight, wt.%) [83].

Component/Element	Acid Process Lithium Slag	Alkali Process Lithium Slag	Salt-Roasting Lithium Slag	Notes
Silicon Dioxide (SiO_2)	~60%–70%	~58%–68%	~62%–72%	Main component, exists in the amorphous phase and quartz; core raw material for silica-alumina micro-powder preparation
Aluminum Oxide (Al_2O_3)	15%–20%	14%–18%	16%–21%	Exists in the aluminosilicate phase; participates in hydration reactions when used as a cementitious material
Sulfur Trioxide (SO_3)	~9%–10%	~10%–11%	~8%–9%	Mainly exists in the form of SO_4^{2-} (gypsum phase, $CaSO_4 \cdot 2H_2O$); requires desulfurization for building material applications
Calcium Oxide (CaO)	3%–5%	4%–6%	2%–4%	Derived from limestone neutralization (acid process) or alkali additives (alkali process); promotes hydration in cement systems
Magnesium Oxide (MgO)	0.5%–1.2%	0.3%–0.8%	0.4%–1.0%	Trace impurity; low content, no significant impact on mainstream utilization
Iron Oxide (Fe_2O_3)	<0.5%	<0.5%	<0.5%	Trace impurity; controlled via magnetic separation in silica-alumina micro-powder production
Lithium Oxide (Li_2O)	0.1%–0.3%	0.08%–0.25%	0.12%–0.35%	Residual unextracted lithium; recyclable via advanced leaching technologies (e.g., bio-leaching)
Tantalum Pentoxide (Ta_2O_5)	0.01%–0.03%	0.008%–0.025%	0.012%–0.032%	Exists in the tantalite-niobite phase; recoverable via Falcon centrifugal gravity separation + magnetic separation
Niobium Pentoxide (Nb_2O_5)	0.005%–0.02%	0.004%–0.018%	0.006%–0.022%	Coexists with Ta; separation requires differential shaking table gravity separation due to similar chemical properties
Potassium Oxide (K_2O)	0.8%–1.5%	0.5%–1.0%	1.2%–2.0%	Higher in salt-roasting slag (from potassium sulfate additive); may affect concrete setting time
Sodium Oxide (Na_2O)	0.3%–0.8%	1.0%–1.8%	0.4%–0.9%	Higher in alkali-process slag (from sodium carbonate); improves the reactivity of silica-alumina components
Other Impurities (MnO, TiO_2, etc.)	<0.5%	<0.5%	<0.5%	Trace elements; leaching concentration below hazardous waste limits, no environmental risk

5. Resource Utilization Scheme of Lithium Slag

The increasing demand for lithium resources has resulted in the production of large quantities of lithium slag [84]. At present, lithium slag is only partially used in building materials such as cement or concrete, and most of it is processed in the form of accumulation or landfill.

5.1. Gypsum

Lithium slag produced during the smelting process of spodumene contains a certain amount of gypsum, and gypsum can be effectively separated through flotation technology to achieve resource utilization [85]. Lithium slag has high chemical activity and certain gelling properties, which make it potentially applicable in gypsum production. Studies have shown that the active ingredients in lithium slag can react with calcium carbonate in gypsum to generate hydration products with a certain strength, which can effectively

utilize the valuable components in lithium slag. Mixing lithium slag with natural gypsum can produce gypsum products with good performance. Studies have shown that mixing lithium slag with natural gypsum can produce gypsum boards with high strength and durability [86]. In addition, lithium slag can also be used to produce gypsum-based building materials, such as gypsum blocks, gypsum putty, etc.

In terms of market scale, the annual demand for building gypsum in China exceeds 50 million tons [87], while there is a shortage of industrial by-product gypsum. Based on the calculation of 120 million tons of annual lithium slag output in China and a gypsum content of 7%–8% in lithium slag, 8–10 million tons of gypsum can be converted from lithium slag annually, which can fill 16%–20% of the aforementioned supply gap, showing great potential in supplementing gypsum supply. Furthermore, gypsum produced from lithium slag must comply with the national standard GB/T 9776-2008 (Gypsum and Gypsum Products) [88], which specifies that the SO_3 content in gypsum boards shall not exceed 4.5%. However, the SO_3 content of gypsum separated from lithium slag is usually 9%–10%, so moderate desulfurization treatment (e.g., adding 5%–8% limestone powder) is required. Although this treatment increases the unit cost by 15–20 CNY/ton, it does not affect the overall economic viability of the process.

Gypsum slag-based cementitious materials are a type of hydraulic cementitious material made by mixing and grinding granulated blast furnace slag, gypsum, and alkaline activators (such as cement clinker and quicklime) as the main raw materials [89]. They have high compressive strength, low hydration heat, and excellent resistance to sulfate attack.

Zeng et al. [90] investigated the effects of industrial solid wastes such as lithium slag on the properties of gypsum slag-based cementitious materials. The hydration and hardening properties of the cementitious material system after the addition of solid waste were studied using characterization methods such as XRD, SEM, and TG-DTG (Figure 12). The results show that in the low-carbon gypsum slag-based cementitious material system, the main hydration products are AFt, C-S-H gels, and CH, which are formed through the mutual activation of slag, gypsum, and alkali. As hydration progresses, the reactivity of the solid waste materials is fully activated. Under the synergistic action of slag, more AFt and C-S-H gels are generated via gypsum consumption. Meanwhile, the reactive components of each material also participate in secondary hydration reactions with CH. Various hydration products are interweaved into a very dense microstructure, filling the pores of the paste and enhancing the strength of the gypsum slag-based cementitious system. This is also beneficial for the recycling and utilization of lithium slag.

Dong et al. [91] proposed a combined process of "gradient flotation–low-temperature impurity removal", which solves the separation problem caused by the tight intergrowth of gypsum and aluminosilicate minerals in lithium slag and breaks through the bottlenecks of low purity and high reagent consumption seen in traditional flotation. Under the conditions of a pH of 7.5–8.0 and a collector dosage of 120 g/t, the grade of the gypsum concentrate is increased to over 92%, with a recovery rate of 88% (15 percentage points higher than that of conventional flotation). Residual lithium salts are removed by low-temperature (80–90 °C) water washing, reducing the Li_2O content in the concentrate to below 0.15% and avoiding efflorescence in subsequent products. XRD and SEM analyses confirm that a hydrophobic adsorption layer is formed on the gypsum surface during the flotation process, while aluminosilicate minerals remain hydrophilic due to the action of depressants, thus achieving efficient separation.

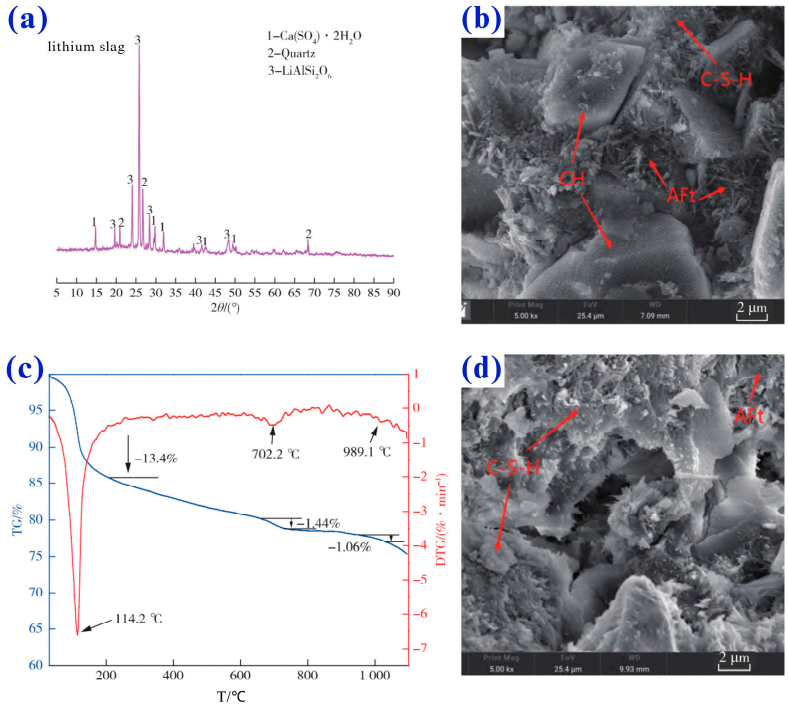


Figure 12. (**a**) XRD patterns of raw materials; (**b**) SEM morphologies of different slag samples after three days of hydration; (**c**) TG and DTG curves of different slag samples at a hydration age of 28 days; (**d**) SEM morphologies of different slag samples after 28 days of hydration [90].

5.2. Silicon–Aluminum Powder

The silicon–aluminum micro-powder in lithium slag is a high-value-added non-metallic material, with its main components being SiO_2 and Al_2O_3 [92], and has shown good application prospects in multiple fields. In the field of building materials, the silicon–aluminum micro-powder can be used as a concrete admixture to replace part of the cement, thereby improving the strength and durability of concrete. Compared with conventional supplementary cementitious materials (SCMs), such as fly ash and granulated blast furnace slag, when a lithium slag silicon–aluminum micro-powder replaces 15%–20% of cement [93], the 28-day compressive strength of concrete is 5%–8% higher than that of fly ash-admixed concrete (under the same replacement rate) and 3%–5% higher than that of granulated blast furnace slag-admixed concrete; however, its 3-day early strength is 10%–12% lower than that of the latter two, which can be improved by adding 1%–2% sodium silicate as an alkaline activator.

In terms of industrial applications, the silicon–aluminum micro-powder can be used in the production of glass fibers to replace natural pyrophyllite, further reducing production costs. The main components of glass fibers include SiO_2, Al_2O_3, CaO, and MgO, among others [94], which account for about 90% of the total composition of glass fibers. These components are primarily derived from natural mineral raw materials, such as quartz sand, pyrophyllite, kaolin, dolomite, and borocalcite. The primary components of lithium-bearing silicon–aluminous micro-powders are SiO_2 and Al_2O_3, with relatively high mass fractions that can meet the requirements for silicon–aluminous raw materials in industries such as glass fibers and ceramics. Thanks to advanced separation and purification processes, the mass fractions of iron (Fe_2O_3) and sulfur (SO_3) in lithium-bearing silicon–aluminous micro-powders are low. This low impurity content provides an advantage in applications with high purity requirements.

Economically, the production cost of lithium-bearing silica-aluminum micro-powders (including grinding, magnetic separation purification, and drying) is 200–300 CNY/ton, 40–50% lower than the market price of the natural pyrophyllite (500–600 CNY/ton) used

in glass fiber production. China's annual demand for glass fiber raw materials is approximately 8 million tons; lithium slag can supply 1.2–1.5 million tons of qualified silica-aluminum micro-powder annually, with a potential market share of 15%–19%. Regulatory barriers are minimal, as toxic element tests (e.g., Pb and Cd) confirm that the micro-powder meets environmental protection standards for building and industrial materials. Wang et al. [95] found that a lithium-bearing silicon-aluminous micro-powder, as a new type of raw material, has the potential to replace pyrophyllite as a raw material for glass fibers. It exhibits good performance with regard to both physical and chemical properties and processing characteristics. Moreover, the test results for toxic and harmful elements indicate that neither the glass batch nor the glass samples contain toxic or harmful substances, meeting environmental protection requirements. Therefore, we believe that further exploration of the application of lithium-bearing silicon–aluminous micro-powders in actual production is warranted, and related processes should be optimized to achieve a higher production efficiency and better product performance.

Silicon–aluminum micro-powder composite materials have the advantages of a low density, high thermal conductivity, and a low thermal expansion coefficient, as well as great potential in applications such as aerospace, aviation, and national defense. Zhaoyang Kong et al. [96] focused on the study of high-silicon–aluminum composite materials with a silicon content of 60%. They used ball milling to pre-treat the powders, and the most ideal results were achieved when the ball milling time was 8 h, the ball-to-powder ratio was 10:1, and the ball milling speed was 200 revolutions per minute (r/min). The morphology of the original powders (i.e., Al powder and Si powder) used in this study is shown in Figure 13. Under the aforementioned optimal ball milling parameters, the material exhibited excellent properties that meet the standards for electronic packaging materials.

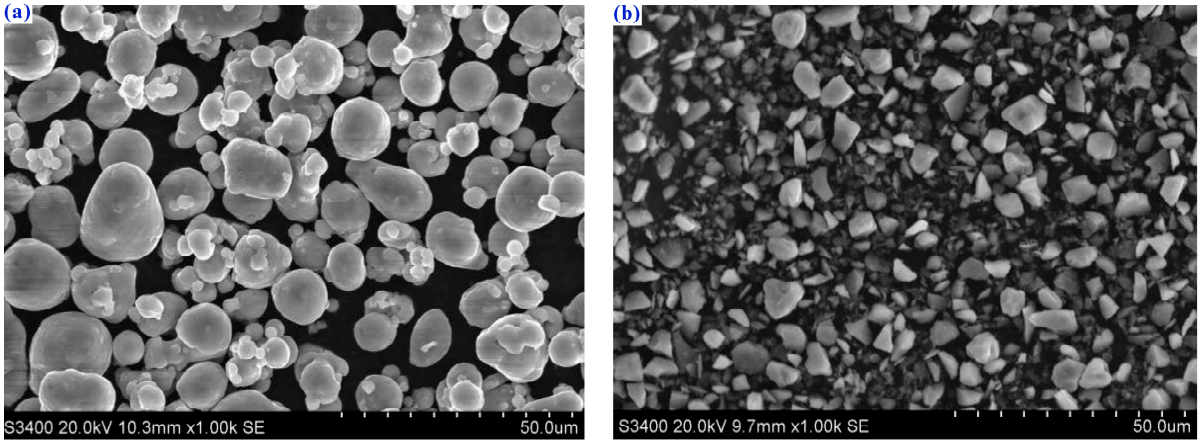


Figure 13. Original powder morphology: (**a**) Al powder, (**b**) Si powder [57].

Regarding environmental protection and sustainability, the resource utilization of lithium slag helps reduce the storage and landfill of solid waste and lower the potential environmental impact [97].

In summary, the silicon–aluminum micro-powder in lithium slag has broad application prospects in multiple fields, including building materials and industrial applications. Through technological innovation and market expansion, the resource utilization of silicon–aluminum micro-powders will help achieve the high-value and sustainable development of lithium slag.

5.3. Fine-Grained Tantalum Concentrate Sludge

Lithium slag contains a wealth of valuable components, among which the fine-grained tantalum-rich mud concentrate has garnered significant attention due to its high content of

tantalum and other rare metals. Tantalum is an important rare metal, widely used in fields such as electronics, aerospace, and chemical engineering. Therefore, the efficient recovery of tantalum from lithium slag holds important economic and environmental significance. Tantalum primarily exists in lithium slag in the form of tantalates, which are characterized by high chemical stability and corrosion resistance. Studies have shown that, although the tantalum content in lithium slag is relatively low, it can be efficiently recovered through appropriate processes.

Regarding tantalum recovery technologies, flotation requires large doses of collectors (e.g., oleic acid) and is inefficient for −75 μm fine particles (tantalum recovery <70%), whereas the Falcon centrifugal gravity separation–magnetic separation process achieves 85.70% Ta recovery for fine-grained lithium slag. Hydrometallurgical recovery from tin slags relies on strong acid leaching (e.g., 40% HCl) and generates toxic heavy metal-containing wastewater, while lithium slag tantalum separation uses physical methods (no chemical reagents), reducing environmental treatment costs. However, lithium slag has a lower tantalum grade (0.01–0.03% Ta_2O_5) than tin slags (0.1%–0.5% Ta_2O_5), requiring pre-enrichment (via Falcon centrifugation) to ensure economic viability. Nevertheless, the low impurity content (Fe_2O_3 < 0.5%) of lithium slag-derived tantalum concentrate improves its downstream processing value.

Tantalum (Ta) and niobium (Nb) are widely used in fields such as electronics and aerospace due to their high melting points and corrosion resistance. However, they are chemically similar and often found in the same ores, making their separation challenging.

Deng et al. [98] have developed a combined process of "high-intensity magnetic separation for tailing discarding–size-fractionated secondary tailing discarding–differentiated shaking table gravity separation". This process enables the efficient recovery of the rare metals tantalum (Ta) and niobium (Nb) from the waste residue generated after lithium extraction from spodumene in a certain area of Sichuan, providing a new technical pathway for the resource utilization of industrial solid waste. The main target minerals in the lithium slag are tantalum–niobium minerals, which are mainly composed of tantalite–niobite, with small amounts of microlite, manganotantalite, etc. Under the microscope, a small number of tantalum–niobium mineral particles exist as monomers, while most are embedded in the glass phase or intergrown with the glass phase and aluminosilicates, as shown in Figure 14.

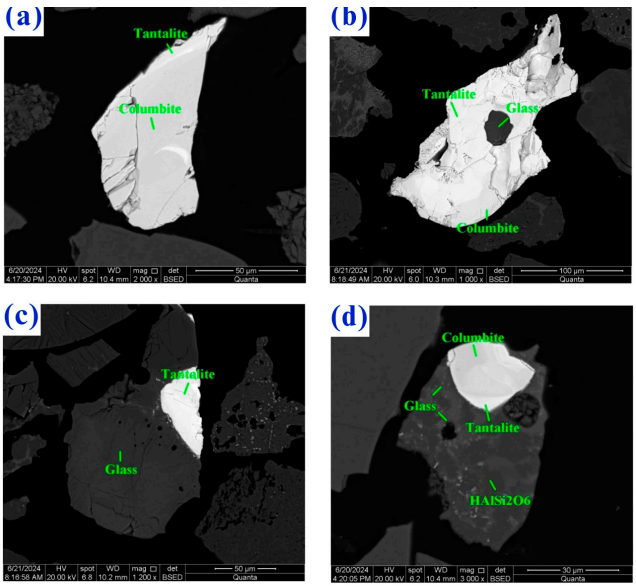


Figure 14. (**a**) The monomer particles of tantalite–columbite, (**b**) tantalite intergrowth with glass, (**c**) tantalite–columbite intergrowth with glass and aluminosilicate, and (**d**) microlite encapsulated in the glass phase [98].

The recycling and utilization of tantalum not only improve resource utilization efficiency but also reduce dependence on natural tantalum ores. Tantalum is a rare metal with a high melting point, high hardness, and excellent corrosion resistance, and it is widely used in fields such as electronics, aerospace, and chemical engineering. Recovering tantalum from lithium slag can not only meet market demand but also reduce environmental pressure.

5.4. Challenges Faced by the Application of the Lithium Slag Resource

Lithium slag has a complex chemical composition, often containing not only lithium compounds but also various impurities such as calcium, magnesium, iron, and aluminum oxides. Moreover, its composition and properties may vary significantly depending on the production process of lithium products and the source of raw materials, which makes it difficult to establish a unified and stable application technology system. It is difficult to efficiently separate and recover valuable components in lithium slag. The separation of lithium from other metal ions usually requires sophisticated separation technologies and equipment. Existing separation methods, such as chemical precipitation and solvent extraction, may face issues such as low separation efficiency, high cost, and poor selectivity. Although some comprehensive utilization technologies regarding lithium slag have been developed, most of them are still in the laboratory or pilot-scale stage, and there are few mature large-scale industrial application technologies. The transformation and application of these technologies in actual production often face problems such as high investment costs, complex operations, and poor economic benefits, resulting in the low overall utilization rate of lithium slag resources.

To address the above challenges and promote the large-scale, high-value utilization of lithium slag, the following research priorities are proposed:

Develop integrated flowsheets combining lithium extraction and slag valorization: For example, integrate microwave-assisted acid roasting (for lithium extraction) with the in situ separation of silica-aluminum micro-powders, reducing intermediate material transportation and energy consumption, and explore the co-extraction of lithium and rare metals (Ta/Nb) during the slag treatment process to improve overall resource efficiency.

Improve the selectivity of lithium recovery from multi-component solutions: Focus on developing high-selectivity adsorbents (e.g., lithium-ion sieves modified with functional groups) to address the low separation efficiency of Li^+ from coexisting ions (Mg^{2+} and Ca^{2+}) in lithium slag leachate, and optimize solvent extraction systems (e.g., using ionic liquids as extractants) to reduce reagent consumption and environmental impact.

Perform life cycle assessments (LCAs) to quantify environmental benefits: Establish LCA models covering the entire chain of lithium slag "generation → treatment → utilization", comparing the environmental impacts (GHG emissions, water consumption, and soil pollution) of different utilization routes (e.g., building materials vs. rare metal recovery) with traditional landfill disposal, and provide data support for formulating targeted environmental policies.

Establish standardized technical systems: Develop industry standards for lithium slag utilization in typical fields (e.g., "Technical Specification for Lithium Slag Used in Cementitious Materials"), clarifying index requirements (SO_3 content and particle size distribution) and testing methods, and construct a database of lithium slag properties from different extraction processes to guide process-specific utilization.

6. Conclusions and Future Recommendations

Spodumene constitutes one of the primary lithium ore resources in the contemporary industrial sector. Owing to its relatively simple chemical composition and high lithium

grade, it exhibits favorable processability for lithium extraction. Currently, the mainstream technical routes for lithium extraction from spodumene predominantly include acid leaching, alkali decomposition, salt roasting, and chlorination roasting. Each of these processes possesses distinct advantages and inherent limitations. For instance, the sulfuric acid leaching method, as a mature and industrially validated technology, is constrained by the generation of sulfate-containing residues; in contrast, the chlorination roasting process features rapid reaction kinetics but imposes stringent requirements on equipment corrosion resistance and operational safety standards.

With the rapid expansion of the lithium-ion battery industry, the resource utilization of lithium slag—a key by-product derived from the spodumene lithium extraction process—has emerged as a research focus in related fields. Lithium slag is enriched with multiple high-value components, such as tantalum (Ta), niobium (Nb), silica-alumina micro-powder, and gypsum, endowing it with significant potential for resource recovery. Nevertheless, the current disposal strategies for lithium slag remain dominated by open-air stockpiling and landfilling. This conventional approach not only leads to the waste of valuable resources but also poses the potential risks of soil and groundwater contamination, thereby triggering environmental concerns.

Existing research findings demonstrate that lithium slag exhibits promising application prospects in the domains of building material fabrication, geopolymer material development, and glass production. However, the residual sulfate components in lithium slag—primarily originating from the sulfuric acid leaching process—have become a critical bottleneck restricting its large-scale and high-value utilization. In parallel, technological advancements in the recovery of strategic metals (e.g., Ta and Nb) from lithium slag are continuously progressing, providing new avenues for their comprehensive resource utilization.

In conclusion, remarkable advancements have been achieved in the realms of technological innovation, green process development, and integrated utilization regarding spodumene-based lithium extraction and lithium slag resource recycling. Looking ahead, with the continuous optimization of core technologies and reinforcement of policy support, the processes of lithium extraction from spodumene and lithium slag resource utilization are anticipated to become more efficient and achieve low-carbon and sustainable development. This will ultimately offer robust technical and resource support for the advancement of the new energy industry and its upstream and downstream industrial chains.

To address current bottlenecks and drive the industrial application of lithium slag utilization, the following actionable research priorities are proposed:

Pilot-scale demonstration projects for slag utilization technologies: Focus on two high-potential routes: (1) “lithium slag gypsum + cementitious materials” (targeting 100,000-ton/year production lines to verify the stability of SO_3 control and mechanical performance), and (2) “fine-grained tantalum concentrate recovery from lithium slag” (building 5000-ton/year pilot plants to optimize Falcon centrifugal–magnetic separation parameters and reduce energy consumption by 15%–20%). These projects will bridge the gap between laboratory research and industrial application, providing scalable technical templates.

Optimization of slag composition during lithium extraction: Adjust extraction process parameters to improve downstream recyclability. For example, in the sulfuric acid method, control roasting temperature (950–1000 °C) and acid dosage (1.2–1.3 times the theoretical requirement) to reduce the residual SO_3 in lithium slag from 9%–10% to 5%–6%; in the alkali method, optimize the Na_2CO_3 recycling rate (>90%) to reduce the Na^+ content in slag, enhancing compatibility with concrete admixtures.

Development of green leaching agents for lithium slag valorization: R&D focus on low-toxicity, recyclable agents, such as (1) bio-leaching systems (using *Acidithiobacillus ferrooxidans* to extract residual Li^+ from slag, reducing acid consumption by 40%), and (2) deep eutectic solvents (DESs) for the selective separation of Ta/Nb, avoiding heavy metal pollution from traditional hydrometallurgical reagents.

Author Contributions: Y.B.: supervision, project administration, funding acquisition, and writing—review and editing. W.Y.: methodology, investigation, and writing—original draft. S.H.: data curation, investigation, and visualization. X.D.: formal analysis and resources. A.S.: formal analysis. Q.G.: formal analysis and resources. S.Z.: methodology. W.P.: investigation. W.W.: formal analysis. P.G.: formal analysis. Y.Y.: formal analysis. All authors have read and agreed to the published version of the manuscript.

Funding: This work was supported by the National Natural Science Foundation of China (Grant No. 52304287, Grant No. U23A20602), the Natural Science Foundation of Hunan Province (Grant No. 2023JJ50232), and the Scientific Research Project of Hunan Education Department (Grant No. 22A0337).

Data Availability Statement: The original contributions presented in this study are included in the article. Further inquiries can be directed to the corresponding authors.

Acknowledgments: This study was supported by the National Natural Science Foundation of China, the Natural Science Foundation of Hunan Province, and the scientific research program of Hunan Provincial Department of Education.

Conflicts of Interest: The authors declare no conflicts of interest.

References

1. Han, R.Q. Research on the Synergistic Effect of Continuous Mergers and Acquisitions of Enterprises from the Perspective of Resource Allocation—Take Tianqi Lithium as an Example. Master's Thesis, Shanxi University of Finance & Economics, Taiyuan, China, 2024.
2. Han, M.Y. Synthesis of Aluminum Salt Adsorbent by Solvothermal/Hydrothermal Method and Its Lithium Extraction Performance. Master's Thesis, Dalian University of Technology, Dalian, China, 2025.
3. Zhai, Q.L.; Cao, Z.Q.; Liu, R.Q.; Song, Y.F.; Sun, W. Advances in Spodumene Beneficiation and Metallurgical Technologies. *Nonferrous Met. (Miner. Process. Sect.)* **2025**, *77*, 23–41. [CrossRef]
4. Zhang, Z.; Qin, Y.; Sun, X. Lithium Material Flow Analysis in International Trade: A Life Cycle Perspective. *Trans. Nonferrous Met. Soc. China* **2025**, *35*, 1362–1380. [CrossRef]
5. Habib, K.; Hansdóttir, S.T.; Habib, H. Critical Metals for Electromobility: Global Demand Scenarios for Passenger Vehicles, 2015–2050. *Resour. Conserv. Recycl.* **2020**, *154*, 104603. [CrossRef]
6. Tarascon, J.-M. Is Lithium the New Gold? *Nat. Chem.* **2010**, *2*, 510. [CrossRef]
7. Wang, D.; Dai, H.; Liu, S.; Wang, C.; Yu, Y.; Dai, J.; Liu, L.; Yang, Y.; Ma, S. Research and Exploration Progress on Lithium Deposits in China. *China Geol.* **2020**, *3*, 137–152. [CrossRef]
8. Cheng, F.Q.; Zhou, N.; Nouman, N.M.; Cui, L.; Yin, C.X. Classification and Progress of Extraction Technologies for Nonferrous Metal Resources. *Sci. China Chem.* **2025**, *68*, 458–474. [CrossRef]
9. Liu, X.; Lin, Y.; Yue, B.; Meng, B.B.; Cheng, L.Y.; Zhang, M.Y. Physicochemical Properties Analysis of Leaching Slag Generated in the Process of Lithium Salt Production from Lepidolite. *Chin. J. Environ. Eng.* **2025**, *19*, 1723–1729.
10. Zou, J.Z.; Lin, L.P.; Cheng, S.P.; Wang, X.; Guobiao, L.; Wang, D. Research Progress on the Preparation of Lithium Slag Lightweight Aggregate. *Mod. Chem. Res.* **2025**, *15*, 28–30. [CrossRef]
11. Zhang, S.J.; Yang, S.Q.; Che, C.Y.; Ma, R.T. Research on the Preparation and Mechanical Properties of Alkali-Activated Lithium Slag-Based Composite Paste Backfill Material Using RSM-BBD. *J. Min. Saf. Eng.* **2025**, *42*, 1141–1152. [CrossRef]
12. Xiong, H.M.; Sun, J.R.; Liu, C.P.; Xian, W.; Wang, W.Q.; Luo, L.T.; Li, S. Study on Sintering Behavior and Properties of Lithium Slag-Based Foamed Ceramics. *J. Non-Cryst. Solids* **2023**, *617*, 122499. [CrossRef]
13. Wu, Y.W.; Zhang, L.; Wang, K.; Chen, X.L.; Li, J.R. A Brief Analysis of China's Industrial Solid Waste Resources and Phosphogypsum Utilization Policy. *Chem. Eng. Manag.* **2025**, *13*, 53–55. [CrossRef]

14. Li, Y.N.; Wu, S.M.; Chen, L.T.; Fan, H.S.; Zhang, Y.F.; Zeng, L.X. Multiple Yolks-Shell Cobalt Phosphosulfide Nanocrystals Encapsulating into Rich Heteroatoms Co-Doped Carbon Frameworks for Advanced Sodium/Potassium Ion Batteries. *Chin. Chem. Lett.* **2025**, *36*, 706–711. [CrossRef]
15. Li, X.; Hou, L.; Li, Z.; Jin, R.; Li, Y.; Shuming, R.A.N. Lithium Resources in Brine of China's Sea Salt Field Operations. *Acta Geol. Sin. (Eng.)* **2016**, *90*, 767–768. [CrossRef]
16. Zhu, Y.F. Extracting Lithium from Salt-Lake Brine. *Nat. Chem. Eng.* **2024**, *1*, 725. [CrossRef]
17. Yang, M.L.; Zhong, Y.C.; Liu, X.F.; Wang, S.C.; Qu, T. Review of Technologies to Extract Lithium from Hard Rock Lithium Minerals. *Miner. Eng.* **2025**, *232*, 109577. [CrossRef]
18. Xie, R.Q.; Zhao, Z.H.; Tong, X.; Xie, X.; Song, Q.; Fan, P.Q. Review of the Research on the Development and Utilization of Clay-Type Lithium Resources. *Particuology* **2024**, *87*, 46–53. [CrossRef]
19. Deng, Y.; Chai, G.L.; Zhang, Y.H. Research Progress on Lithium Extraction from Salt-Lake Brine. *J. Ind. Eng. Chem.* **2025**, *148*, 92–108. [CrossRef]
20. Wu, C. Discussion on Rational Development of Lithium Resources in Qinghai Salt Lake. *Qinghai Sci. Technol.* **2017**, *24*, 25–31.
21. Johnson, C.A.; Clavijo, A.; Lorca, M.; Andrade, M.O. Bringing the State Back in the Lithium Triangle: An Institutional Analysis of Resource Nationalism in Chile, Argentina, and Bolivia. *Extr. Ind. Soc.* **2024**, *20*, 101534. [CrossRef]
22. Pu, X.H.; Du, X.H.; Wang, G.C.; Zhang, Y.; Wang, Q.; Wu, H. Preparation and Adsorption Performance Study of H2TiO3 Lithium Ion Sieve with Industrial Metantitanic Acid as Raw Materia. *Multipurp. Util. Miner. Resour.* **2021**, *4*, 176–181.
23. Zhao, W.; Zheng, M.P. The Research of Chinese Salt Lake Organisms: History, Status and Expectation. *Acta Geol. Sin. Engl. Ed.* **2014**, *88*, 121–122. [CrossRef]
24. Zhao, Y.J.; Hu, Y.F.; Shen, L.J.; Liu, W.P.; Jiao, J.; Jiao, P.C.; Liu, C.L. Santosh Pathways and Mechanisms of Lithium Enrichment in Brine Deposits: Geochemical and Isotopic Evidence from the Bieletan Section in the Qaidam Basin, Northwestern China. *J. Earth Sci.* **2024**, 1–37.
25. Herrera, C.; Urrutia, J.; Godfrey, L.; Jódar, J.; Pereira, M.; Villarroel, C.; Durán, C.; Soto, I.; Lam, E.J.; Gómez, L. An Evaluation of the Brine Flow in the Upper Part of the Halite Nucleus of the Salar de Atacama (Chile) through an Isotopic Study of δ 18 O and δ2H. *Water* **2024**, *16*, 2651. [CrossRef]
26. Zhu, R.; Wang, S.X.; Srinivasakannan, C.; Li, S.W.; Yin, S.H.; Zhang, L.B.; Jiang, X.B.; Zhou, G.L.; Zhang, N. Lithium Extraction from Salt Lake Brines with High Magnesium/Lithium Ratio: A Review. *Env. Chem. Lett.* **2023**, *21*, 1611–1626. [CrossRef]
27. Lucrecia López Steinmetz, R.; Salvi, S.; García, M.G.; Arnold, Y.P.; Béziat, D.; Franco, G.; Constantini, O.; Córdoba, F.E.; Caffe, P.J. Northern Puna Plateau-Scale Survey of Li Brine-Type Deposits in the Andes of NW Argentina. *J. Geochem. Explor.* **2018**, *190*, 26–38. [CrossRef]
28. Tran, K.T.; Han, K.S.; Kim, S.J.; Kim, M.J.; Tran, T. Recovery of Magnesium from Uyuni Salar Brine as Hydrated Magnesium Carbonate. *Hydrometallurgy* **2016**, *160*, 106–114. [CrossRef]
29. Lin, S.N.; Zhang, T.A.; Pan, X.J.; Zhang, J.J. Eco-Friendly Extraction of Magnesium and Lithium from Salt Lake Brine for Lithium-Ion Battery. *J. Clean. Prod.* **2021**, *327*, 129481. [CrossRef]
30. Bian, S.J.; Liu, X.; Gao, D.D.; Hao, Y.; Li, W. Study on Natural Evaporation Process of Longmucuo Brine. *AMR* **2013**, *807–809*, 2408–2412. [CrossRef]
31. Zhu, X.; Yue, H.; Sun, W.; Zhang, L.; Cui, Q.; Wang, H. Study on Adsorption Extraction Process of Lithium Ion from West Taijinar Brine by Shaped Titanium-Based Lithium Ion Sieves. *Sep. Purif. Technol.* **2021**, *274*, 119099. [CrossRef]
32. Guo, X.Y.; Hu, S.F.; Wang, C.X.; Duan, H.H.; Xiang, X. Highly Efficient Separation of Magnesium and Lithium and High-Valued Utilization of Magnesium from Salt Lake Brine by a Reaction-Coupled Separation Technology. *Ind. Eng. Chem. Res.* **2018**, *57*, 6618–6626. [CrossRef]
33. Nie, Z.; Bu, L.; Zheng, M. Lithium Resources Industrialization of Salt Lakes in China: A Case Study of the Xitaijinaier Salt Lake and the Zabuye Salt Lake. *Acta Geosci. Sin.* **2010**, *31*, 95–101.
34. Tadesse, B.; Makuei, F.; Albijanic, B.; Dyer, L. The Beneficiation of Lithium Minerals from Hard Rock Ores: A Review. *Miner. Eng.* **2019**, *131*, 170–184. [CrossRef]
35. Dessemond, C.; Lajoie-Leroux, F.; Soucy, G.; Laroche, N.; Magnan, J.-F. Spodumene: The Lithium Market, Resources and Processes. *Minerals* **2019**, *9*, 334. [CrossRef]
36. Li, H.S.; Zhu, T.; Chen, X.S.; Liu, H.B.; He, G.S. Improving China's Global Lithium Resource Development Capacity. *Front. Environ. Sci.* **2022**, *10*, 938534. [CrossRef]
37. Petrakis, E.; Alexopoulos, I.; Pantelaki, O.; Karmali, V.; Komnitsas, K. Advances in Mineral Processing of Hard-Rock Lithium Ores: A Comprehensive Review. *Min. Metall. Explor.* **2025**, *42*, 1251–1283. [CrossRef]
38. Kirk, R.D.; Newsome, L.; Falagan, C.; Karen, A. Hudson Edwards Bioleaching of Lithium from Jadarite, Spodumene, and Lepidolite Using Acidiothiobacillus Ferrooxidans. *Front. Microbiol.* **2024**, *15*, 1467408. [CrossRef] [PubMed]
39. Maistry, N.; Singh, A. HLS Testwork on Spodumene and Lepidolite Samples to Determine Maximum Achievable Lithium Upgrade. *Minerals* **2025**, *15*, 396. [CrossRef]

40. Ren, W.K.; Liu, Z.K.; Wang, Q.Y.; Ma, Y.L.; Hou, D.B.; He, M.Y.; Zhou, J.D.; Cheng, Y.Y.; Li, Z.Y.; Rao, H.H.; et al. Research Progress on the Important Characteristics, Metallogenic Conditions and Formation Mechanism of Clay-Type Lithium Deposits and Resource Extraction Technology. *J. Salt Lake Res.* **2025**, *33*, 69–90. [CrossRef]
41. Zhou, H.D.; Liu, Y.B.; Ma, B.Z.; Wang, C.Y.; Chen, Y.Q. Efficient Lithium Extraction from Low-Grade Clay-Type Lithium Ore via Nitric Acid Pressure Leaching. *J. Environ. Chem. Eng.* **2025**, *13*, 118653. [CrossRef]
42. Shen, Y.H.; Yang, W.L. Spatial-Temporal Pattern Evolution of Global Lithium Trade Network and China 's Status from the Perspective of Industrial Chain. *J. Inn. Mong. Univ. Financ. Econ.* **2025**, *23*, 81–92. [CrossRef]
43. Pan, Z.S.; Zhang, Z.Z.; Wu, Q. Analysis of Potash Supply and Demand in China from 2024 to 2035: Based on the Study of Geological Characteristics of Mineral Deposits. *Acta Geol. Sin.* **2024**, *98*, 2989–3001. [CrossRef]
44. Liu, X.; Wang, C.L.; Liu, X.L.; Liu, S.H.; Liu, D.H.; Yan, K.; Liu, S.H.; Liu, Y.T. Main Types, Distribution, Development and Utilization of Lithium Deposits in China. *Geol. China* **2024**, *51*, 811–832.
45. Zheng, M.; Xing, E.; Zhang, X.; Li, M.; Che, D.; Bu, L.; Han, J.; Ye, C. Classification and Mineralization of Global Lithium Deposits and Lithium Extraction Technologies for Exogenetic Lithium Deposits. *China Geol.* **2023**, *6*, 547–566.
46. Zheng, M.P.; Zheng, Y.; Liu, J. The New Discoveries of Saline Lakes and Geothermal Ore Deposits on the Qinghai-Tlbet Plateau. *Acta Geosci. Sin.* **1990**, *11*, 151.
47. Zhao, Y.Y.; Fu, J.J.; Li, Y. Super Large Lithium and Boron Deposit in Jadar Basin, Serbia. *Geol. Rev.* **2015**, *61*, 34–44. [CrossRef]
48. Wang, Q.; Yuan, C.; Xu, H. Analysis of the global lithium resource distribution and potential. *China Min. Mag.* **2015**, *24*, 10–17. [CrossRef]
49. Yuan, X.J. Demand Forecast and Supply Analysis of Critical Mineral Required by New Energy Vehicles. Master's Thesis, China University of Geosciences, Wuhan, China, 2020.
50. Ma, J.; Hong, T.; Gao, H.H.; Wei, P.T. 'Lithium' Unlocks Future Energy Passwords. *Bull. Mineral. Petrol. Geochem.* **2022**, *41*, 687–692. [CrossRef]
51. Lai, X.; Chen, C.H.; Chen, X.J.; Fei, G.C.; Li, Y.; Wang, J.X.; Cai, Y.H. Process Mineralogy Characteristics of Lijiagou Pegmatite Spodumene Deposit, Sichuan, China. *Minerals* **2023**, *13*, 1180. [CrossRef]
52. Yang, H.P.; Liu, L.; Ding, G.F. Present Situation and Development Trend of Lithium Resources in the World. *Conserv. Util. Miner. Resour.* **2019**, *39*, 26–40. [CrossRef]
53. Wu, Y.G.; Si, X.; Xu, S.P.; Wang, J.Z. Rational Thoughts on Lithium Resources Development and Utilization under New Energy Background. *Resour. Ind.* **2024**, *26*, 90–96. [CrossRef]
54. Gu, T.; Zhang, G.Y.; Wang, Z.Y.; Liu, L.B.; Zhang, L.H.; Wang, W.L.; Huang, Y.L.; Dan, Y.; Zhao, P.; He, Y.; et al. Review: The Formation, Characteristics, and Resource Utilization of Lithium Slag. *Constr. Build. Mater.* **2024**, *432*, 136648. [CrossRef]
55. Han, G.F.; Gu, D.L.; Lin, G.; Cui, Q.; Wang, H.Y. Recovery of Lithium from a Synthetic Solution Using Spodumene Leach Residue. *Hydrometallurgy* **2018**, *177*, 109–115. [CrossRef]
56. Cao, M. Froth Flotation of Spodumene from Spodumene-Bearing Pegmatite Ores: Theoretical and Practical Aspects. Ph.D. Thesis, Central South University, Changsha, China, 2024.
57. Li, W.J.; Nitou, M.V.M.; Zheng, J.Y.; Zhang, Z.Y.; Liu, L.F.; Nie, J.L.; Niu, Y.H.; An, L.; Lv, W.Q. Li-Ion Transport in Solid-State Electrolyte of $Li_{1-x}Al_{1-x}Si_{2+x}O_6$: An Ab Initio Study. *Rare Met.* **2023**, *42*, 2261–2271. [CrossRef]
58. Liu, Y.B.; Ma, B.Z.; Lü, Y.W.; Wang, C.Y.; Chen, Y.Q. A Review of Lithium Extraction from Natural Resources. *Int. J. Miner. Metall. Mater.* **2023**, *30*, 209–224. [CrossRef]
59. Dong, S.H.; Yang, Y.K.; Zhang, H.; Guo, H.; Han, G.H.; Cao, Y.J. Research Progress of Lithium ExtractionTechnology from Spodumene and Crystal Transformation. *Nonferrous Met. (Extr. Metall.)* **2024**, *2*, 48–56.
60. Salakjani, N.K.; Singh, P.; Nikoloski, A.N. Acid Roasting of Spodumene: Microwave vs. Conventional Heating. *Miner. Eng.* **2019**, *138*, 161–167. [CrossRef]
61. Rezaee, M.; Han, S.H.; Sagzhanov, D.; Vaziri Hassas, B.; Slawecki, T.M.; Agrawal, D.; Akbari, H.; Mensah-Biney, R. Microwave-Assisted Calcination of Spodumene for Efficient, Low-Cost and Environmentally Friendly Extraction of Lithium. *Powder Technol.* **2022**, *397*, 116992. [CrossRef]
62. Tian, J.; Ma, S.Y.; Hu, P.; Wang, J.J.; Zheng, X.Y.; Luo, S.S. A Method of Extracting Lithium by Microwave Acid Roasting and Mechanical Ball Milling. U.S. Patent Application No. CN119307715A, 12 September 2024.
63. Zhou, W.C.; Xie, R.Q.; Tong, X.; Xie, X.; Liu, Y.; Zhao, Z.H. Extract Lithium from Clay-Type Lithium Ore by Mixed Acid and Its Mechanism. *Particuology* **2024**, *91*, 323–332. [CrossRef]
64. Gu, H.N.; Guo, T.F.; Wen, H.J.; Luo, C.G.; Cui, Y.; Du, S.J.; Wang, N. Leaching Efficiency of Sulfuric Acid on Selective Lithium Leachability from Bauxitic Claystone. *Miner. Eng.* **2020**, *145*, 106076. [CrossRef]
65. Paris, J.; Mohammadi-Jam, S.; Li, R.H.; Liang, J.Y.; Oh, H.J.; Kökkılıç, O.; Omelon, S.; Waters, K.E. Preliminary Investigation into Lithium Extraction by Phosphoric Acid Leaching of Spodumene. *Miner. Eng.* **2024**, *209*, 108613. [CrossRef]

66. Zhang, J.; Yin, Z.G.; Liang, S.; Deng, X.X.; Zhang, B.Y.; Xu, C.; Tu, M.J.; Gao, Y.B.; Zhan, B.X.; Chang, L.J. A Method for Efficient Extraction of Lithium from Spodumene Clinker and Preparation of Low Iron and Low Sulfur Silicon Aluminum Powder. U.S. Patent Application No. CN118792502A, 17 June 2024.
67. Huo, L.M.; Zhang, J.F.; Dong, H.B. Production and Market Situation of Lithium Hydroxide in China. *China Nonferrous Met.* **2009**, *17*, 74–75.
68. Chen, Y.; Liao, T.; Chen, B.Z.; Tian, Q.Q. Extraction of Lithium from Spodumene by Sodium Carbonate Autoclave Process. *Nonferrous Met. (Extr. Metall.)* **2011**, *9*, 21–23.
69. Tian, Q.Q. Extraction of Lithium Carbonate from Spodumene Ore. Master's Thesis, Central South University, Changsha, China, 2013.
70. Subasinghe, H.C.S.; Rezaee, M. Direct Lithium Extraction from α-Spodumene Using NaOH Roasting and Water Leaching. *Chem. Eng. J.* **2025**, *505*, 159661. [CrossRef]
71. Zhang, X.F.; Tan, X.M.; Liu, W.Z.; Wang, W.; Zhang, L.Z. Current Status and Research Progress of Lithium Extraction Technology from Ore. *Conserv. Util. Miner. Resour.* **2020**, *40*, 17–23. [CrossRef]
72. Liu, C.L.; Qiu, S.B.; Sun, T.Y.; Zhu, M.Q.; Liu, X.; Yu, J.G. A Method for Producing Lithium Sulfate Solution by Spodumene Sulfate Roasting Method. CN114507779A, 9 April 2024.
73. Samoilov, V.I.; Kulenova, N.A.; Sheregeda, Z.V.; Gadylbekova, L.G.; Agapov, V.A.; Shushkevich, L.V. Integrated Processing of Spodumene in Hydrometallurgy. *Russ. J. Appl. Chem.* **2008**, *81*, 494–496. [CrossRef]
74. Chen, L.; Cheng, S.Q.; Qi, Z.P. A Method for Extracting Lithium from Spodumene by Salt Gypsum Assisted Sulfate Method. CN119082493A, 4 April 2025.
75. Chen, Y.; Tian, Q.Q.; Chen, B.Z.; Shi, X.C.; Liao, T. Preparation of Lithium Carbonate from Spodumene by a Sodium Carbonate Autoclave Process. *Hydrometallurgy* **2011**, *109*, 43–46. [CrossRef]
76. Barbosa, L.I.; Valente, G.; Orosco, R.P.; González, J.A. Lithium Extraction from β-Spodumene through Chlorination with Chlorine Gas. *Miner. Eng.* **2014**, *56*, 29–34. [CrossRef]
77. He, Z.G.; Ni, C.Q.; Zhong, H.; Xie, Y.Q. A Method of Mechanical Activation Enhanced Chlorination Roasting of Spodumene for Water Leaching of Lithium. CN118272671A, 29 March 2024.
78. Braga, P.F.A.; Brigido, C.R.D.S.; Pinto, C.P.; França, S.C.A.; Rosales, G.D. Extracting Lithium from Brazilian α-Spodumene via Chlorination Roasting. *Mining* **2025**, *5*, 19. [CrossRef]
79. Wang, Y.R.; Wang, D.M.; Cui, Y.; Zheng, D.P.; Liu, Z. Micro-Morphology and Phase Composition of Lithium Slag from Lithium Carbonate Production by Sulphuric Acid Process. *Constr. Build. Mater.* **2019**, *203*, 304–313. [CrossRef]
80. Tan, H.B.; Zhang, X.; He, X.Y.; Guo, Y.L.; Deng, X.F.; Su, Y.; Yang, J.; Wang, Y.B. Utilization of Lithium Slag by Wet-Grinding Process to Improve the Early Strength of Sulphoaluminate Cement Paste. *J. Clean. Prod.* **2018**, *205*, 536–551. [CrossRef]
81. Qiu, Y.X.; Wu, D.F.; Yan, L.L.; Zhou, Y. Recycling of Spodumene Slag: Preparation of Green Polymer Composites. *RSC Adv.* **2016**, *6*, 36942–36953. [CrossRef]
82. Li, M.S.; Liu, H.; Duan, P.; Ruan, S.Q.; Zhang, Z.H.; Ge, W. The Effects of Lithium Slag on Microstructure and Mechanical Performance of Metakaolin-Based Geopolymers Designed by Response Surface Method (RSM). *Constr. Build. Mater.* **2021**, *299*, 123950. [CrossRef]
83. Xiong, Z.P.; Hu, K.J.; Yuxian, K.; Yan, X.Y.; Li, J.Y. Research Progress on Activation Technology and Mechanism of Lithium Slag. *Mod. Min.* **2024**, *40*, 208–213.
84. Chen, W.; Yu, X.Y.; Jiang, Y. Research Progress on Recycling Technologies of Spent Lithium Iron Phosphate Cathode Materials. *Chin. J. Environ. Eng.* 2025.
85. Yi, P.; Zhang, J.; He, Y.Q.; Yin, Z.G.; Deng, X.X. Test on Flotation Desulfurization of a Lithium Slag in Sichuan. *Mod. Min.* **2023**, *39*, 107–110.
86. Li, C.; Li, J.; Chen, W.Q.; Li, X.Y.; Lu, Z.Y.; Zhan, B.X.; Yang, F.Y.; Hou, L.; Chen, X.M.; Yu, Q.H.; et al. Performance and Hydration of Ternary Compound Cement by Using Lithium Slag, Limestone and Clinker. *Case Stud. Constr. Mater.* **2025**, *22*, e04435. [CrossRef]
87. Xue, L.; Xue, L.T.; Wu, X.Y.; Li, R.; Sun, X.C.; Wu, K.Z.; Chi, R.A. Experimental Study on Hydration Activity Modification of Fluorgypsum. *Bull. Chin. Ceram. Soc.* **2025**, *44*, 223–230. [CrossRef]
88. Zheng, J.G.; Wang, Z.M.; Liu, Y.C. Description of Revised"building Plaster"GB/T 9776—2008. *New Build. Mater.* **2009**, *36*, 13–16. (In Chinese)
89. Ma, F.Y. Study on Preparation and Key Properties of Composite Cementitious Material Containing Phosphogypsum. Master's Thesis, Kunming University of Science and Technology, Kunming, China, 2024.
90. Zeng, L.; Hu, B.; Shi, S. Preparation and Hydration Properties of Multi-Component Solid Waste Low Carbon Cementitious Materials Based on Gypsum and Slag. *Nonferrous Met. (Extr. Metall.)* **2024**, *9*, 154–163.
91. Dong, W.; Zhou, H.L.; Gong, D.D.; Reng, S.L.; Qian, H.L. Research Progress on Resource Utilization Technology of Lithium Smelting Slag. *J. Environ. Eng. Technol.* **2025**, *15*, 308–318.

92. Yang, Y.H.; Liao, S.Y.; Jiang, X.F.; Chen, Y.J.; Zhang, J.; Chen, G. Determination on Beryllium Content in Silicon-Aluminum Powder by Inductively Coupled Plasma Atomic Emission Spectrometry (ICP-AES). *Yunnan Metall.* **2024**, *3*, 155–160, 170.
93. Peng, Z.W. Going Forward by 'Green' and Turning 'Waste' into Treasure. *Mianyang Dly.* **2024**, *6*, 1–2. [CrossRef]
94. Ma, X.Y.; Chen, S.P.; Zhang, Y.J.; Yu, Y.; Yu, H.F.; Wang, B. Study on the Microstructures and Thermophysical Properties of the Spacer Fibre Papers. *China Pulp Pap.* **2025**, *44*, 60–69.
95. Wang, W.N.; Hu, M.R.; Huang, S.L.; Zhang, Y.; Zu, Q.; Huang, S.X. Study on Lithium Silicon Aluminum Powder Replacing Pyrophyllite as Glass Fiber Raw Material. *Fiber Glass* **2025**, *2*, 19–23. [CrossRef]
96. Kong, Z.Y.; Wang, Z.P.; Chen, B.; Li, Y.M.; Li, R.X. Effect of Ball Milling Time on the Microstructure and Properties of High-Silicon–Aluminum Composite. *Materials* **2023**, *16*, 5763. [CrossRef]
97. Tan, H.B.; Li, M.G.; He, X.Y.; Su, Y.; Zhang, J.J.; Pan, H.; Yang, J.; Wang, Y.B. Preparation for Micro-Lithium Slag via Wet Grinding and Its Application as Accelerator in Portland Cement. *J. Clean. Prod.* **2020**, *250*, 119528. [CrossRef]
98. Deng, X.X.; Zhang, J.; He, C.; He, Y.Q.; Yi, P.; Cahng, L.; Yin, Z.G. Experimental Study on Tantalum and Niobium Recovery from Lithium Slag Extracted from Sichuan Spodumene. *Nonferrous Met. (Miner. Process. Sect.)* **2025**, *6*, 83–89. [CrossRef]

Disclaimer/Publisher's Note: The statements, opinions and data contained in all publications are solely those of the individual author(s) and contributor(s) and not of MDPI and/or the editor(s). MDPI and/or the editor(s) disclaim responsibility for any injury to people or property resulting from any ideas, methods, instructions or products referred to in the content.